aerospace

MDPI

Review

Review of Sonic Boom Prediction and Reduction Methods for Next Generation of Supersonic Aircraft

Giordana Bonavolontà *, Craig Lawson and Atif Riaz

Centre for Aeronautics, Cranfield University, Cranfield MK43 0AL, UK; c.p.lawson@cranfield.ac.uk (C.L.); a.riaz@cranfield.ac.uk (A.R.)

* Correspondence: g.bonavolonta@cranfield.ac.uk

Abstract: The reduction of sonic boom levels is the main challenge but also the key factor to start a new era of supersonic commercial flights. Since 1970, a FAA regulation has banned supersonic flights overland for unacceptable sonic booms at the ground, and many research studies have been carried out from that date to understand sonic boom generation, propagation and effects, both on the environment and communities. Minimization techniques have also been developed with the attempt to reduce sonic boom annoyance to acceptable levels. In the last 20 years, the advances in both knowledge and technologies, and companies and institutions' significant investments have again raised the interest in the development of new methods and tools for the design of low boom supersonic aircraft. The exploration of unconventional configurations and exotic solutions and systems seems to be needed to effectively reduce sonic boom and allow supersonic flight everywhere. This review provides a description of all aspects of the sonic boom phenomenon related to the design of the next generation of supersonic aircraft. In particular, a critical review of the prediction and minimization methods found in the literature, aimed at identifying their strengths, limitations and gaps, is made, along with a complete overview of disruptive unconventional aircraft configurations and exotic active/passive solutions to boom level reduction. The aim of the work is to give a clear statement of state-of-the-art sonic boom prediction methods and possible reduction solutions to be explored for the design of next low-boom supersonic aircraft.

Keywords: supersonic aircraft design; sonic boom modeling and prediction; aerodynamics; acoustics

Citation: Bonavolontà, G.; Lawson, C.; Riaz, A. Review of Sonic Boom Prediction and Reduction Methods for Next Generation of Supersonic Aircraft. *Aerospace* **2023**, *10*, 917. https://doi.org/10.3390/aerospace10110917

Academic Editor: Haixin Chen

Received: 27 September 2023
Revised: 20 October 2023
Accepted: 24 October 2023
Published: 27 October 2023

1. Introduction

Since the Wrights brothers' first flight took place in 1903, flying faster has been a human dream, and as research and technology developed, especially with the introduction of jet engines, this dream started to come true. In October 1947, General Charles 'Chuck' Yeager piloted the Bell X-1 [1] to a speed of Mach 1.07, breaking the barrier of sound for the first time and ushering in the era of manned supersonic flight. During the years after this important event, a multitude of supersonic aircraft were manufactured exclusively for military purposes. However, in 1968, the world's first commercial supersonic transport aircraft, the Soviet Tupolev Tu-144, took its first flight, just two months before the inaugural flight of the British–French Concorde. Tupolev Tu-144 was in passenger service in 1977 and 1978 but only on one route, completing just 55 flights. It was a commercial failure with numerous technical faults leading to reliability and safety concerns, culminating in a test flight crash in May 1978. It continued to fly until 1999 as a test vehicle. Concorde was operated from 1976 to 2003, and since that date, no other supersonic transport aircraft has flown. The main reasons for Concorde's limited commercial success were the high fuel consumption linked to the high thrust needed, high operational costs and the impact of the sonic boom produced on the environment and communities. In 1978, an FAA regulation restricted the operation of civil aircraft at speeds greater than Mach 1 overland. This

severely limited the routes viable for Concorde and discouraged the interest in developing new supersonic civil aircraft for a long period of time. This fact if, on one hand, blocked the market for supersonic aircraft, on the other hand raised great interest in the sonic boom phenomenon, and considerable investigation and research, aiming at understanding the phenomenon and predicting it, were undertaken over the following decades. NASA describes the sonic boom as "thunder-like noise a person on the ground hears when an aircraft [. . .] flies overhead faster than the speed of sound" [2]. Sonic boom results from the coalescence of the shock waves generated by an aircraft flying supersonicly trough their propagation into the atmosphere to the ground. Here, a strong and impulsive pressure change is generated that may damage structures and annoy, in a not acceptable way, people. According to Coulouvrat [3], it seems that the sonic booms generating at cruise altitudes are not harmful in terms of intensity, but high adverse reactions might be expected from people likely to be frequently exposed to even low-level booms. It can have a negative impact also on marine and wildlife [4]. The typical sonic boom signature at the ground is the so-called "N-wave" (Figure 1), which is characterized by sharp pressure jumps at the front and back of the waveform, with a slow pressure drop in between. Sonic boom intensity and its extension on the ground depend mainly on aircraft weight, size, altitude and Mach number. The area affected by a sonic boom is called the 'boom carpet' and can extend up to 70 miles behind the aircraft [5].

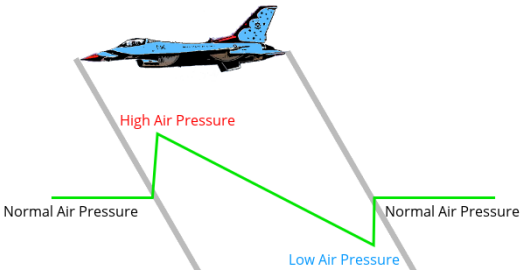

Figure 1. Typical N-wave sonic boom signature at ground (source: [6]).

Several factors, such as variation in signature shape, pressure levels, rise time and frequency content, seem to have a large influence on the resultant sonic booms disturbance level [7]. These are, in turn, affected by environmental conditions, making sonic boom a real complex phenomenon to be analyzed and modeled. In the last 20 years, the encouraging results of the previous studies and research, along with the developments in the aviation industry and the introduction of increasingly advanced technologies, have led many companies to strongly invest in the design and development of the new generation of supersonic aircraft. At the same time, the ICAO (International Civil Aviation Organization) Committee on Aviation Environmental Protection is working to develop new certification standards for supersonic aircraft and environmental regulations in terms of sonic boom, noise and emissions [8]. The FAA is gathering data and information from sonic boom flight test campaigns to determine whether to amend the current ban on supersonic flight by civil aircraft overland in the United States [9]. Sonic boom reduction and mitigation constitutes supersonic flight's biggest challenge. However, the reintroduction of supersonic aircraft needs also to address high efficiency and low climate impact, and must be economically and commercially viable. Although some conventional aircraft designs have proven that they can be carefully shaped and optimized in order to obtain lower levels of both sonic boom and wave drag, it seems to be insufficient to attain sufficient noise reduction. In addition, other stringent requirements on LTO noise, high-altitude NOx emissions and fuel consumption would be difficult to meet. A technological breakthrough is needed for the design of a new generation of supersonic transport aircraft. In order to achieve this, it seems necessary to explore a multitude of different and unconventional aircraft configurations, together with careful airframe–engine integrated design. Provisions should be made, as necessary, for appropriate noise reduction systems and measures, and the evaluation of their impact at the aircraft level is of vital importance. A multi-disciplinary optimization

(MDO) approach is needed, and sonic boom prediction and minimization must be in the loop within the very first steps of the process. In this regard, a review of existing sonic boom prediction methods and mitigation techniques and systems is due.

The paper is organized as follows: Sections 2 deals with a critical review of sonic boom prediction methods and minimization techniques. Section 3 provides an overview of unconventional disruptive aircraft configurations and exotic solutions to reduce and mitigate sonic boom, worth being explored further in the future. Each section includes a critical review paragraph in the end. Conclusions are drawn in Section 4.

2. Sonic Boom Prediction and Minimization

NASA describes sonic boom as a "thunder-like noise a person on the ground hears when an aircraft [...] flies overhead faster than the speed of sound" [2]. Sonic boom results from the coalescence at the ground of strong, impulsive shock waves generated by aircraft flying at supersonic speed. The noise generated on the ground may damage structures and disturb people. Additionally, it can have a negative impact on marine and wildlife [4]. Sonic boom intensity and extension on the ground depends mainly on aircraft weight, size, altitude and Mach number. The area affected by a sonic boom is called the 'boom carpet' and can extend up to 70 miles behind the aircraft [5]. Sonic boom mitigation remains supersonic flight's biggest challenge, and a large number of studies and research projects have been carried out since the 1950s in order to understand the phenomenon and accurately model it. Sonic boom prediction is, in fact, a requirement for both advanced supersonic transport design, and environmental assessment tools of various military and aerospace activities. The problem of sonic boom modeling and prediction can be divided into two main parts: prediction of the near-field pressure signature and its propagation to the ground. The physical domain can be divided into three parts, as shown in Figure 2, according to the pressure signature evolution occurring during its propagation through the atmosphere. Generally, the near-field is considered to be a region small enough that atmospheric gradients do not play a significant role. This is usually a few body lengths. Mid-field is where significant nonlinear distortion of the signature has occurred, but geometric features of the aircraft are still apparent. The far field is where the signature approaches an asymptotic shape [10]. The far-field condition is not always reached at ground: for large aircraft, cruising at high altitudes, in fact, ground signatures can still be mid-field.

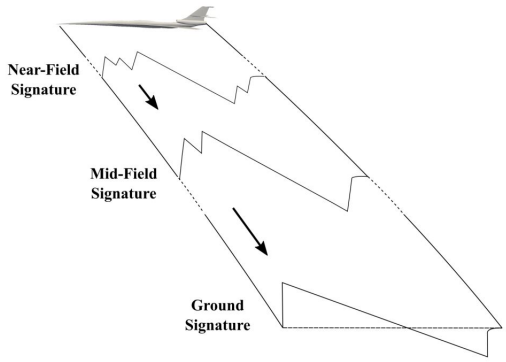

Figure 2. Sonic boom generation, propagation and evolution. Source: [11]).

2.1. Prediction Methods

2.1.1. Fundamental Theory

The fundamental theory for sonic boom modeling and prediction was established in the 1950s with Whitham's works [12,13]. He developed a modified linear theory for the prediction of the sonic boom generated by an axisymmetric non-lifting slender body in a straight supersonic flight at a constant Mach number. The method is based on linearized supersonic flow theory [14] and the supersonic area rule [15,16] for near-field pressure

signature calculation, and the geometrical acoustics method [17] for acoustic propagation. It also accounts for shocks and other nonlinear characteristics existing in real flow and which accumulate as far as one moves away from the body [18] by means of nonlinear steepening and application of the so-called Whitham rule. The effect of wind, density and temperature gradients as well as aircraft maneuvers are included.

Whitham's theory can be summarized in three steps:

1. The acoustic source signature of the vehicle is obtained in terms of a normalized form known as the Whitham F-function. It represents the axisymmetric (or locally axisymmetric) linear acoustic solution in a uniform medium.
2. The F-function is extrapolated to large distances by using geometrical acoustics ray tracing, requiring as inputs the vehicle trajectory and the structure of the atmosphere, and according to which the amplitude changes but the shape is fixed.
3. In the end, Whitham's rule is applied to the complete linear acoustic signature. This accounts for nonlinear steepening or "aging" of the signature. Shocks fitting is carried out such that the total area is conserved ('area balancing' rule).

In 1955, Lomax [19] generalized the modified linear theory for arbitrary lifting configurations, showing that the axisymmetric body area rule can be generalized to asymmetric bodies, including the effects of lift, and Walkden, in 1958, applied these findings to sonic boom prediction [20]. The cross-sectional area distribution $A(x)$ in the F-function (Equation (2)) was substituted by an equivalent area $A_e(x,\theta)$ distribution (which is a function of the azimuthal angle, or angle in the roll direction) comprising both volume and lift contribution (Equation (1)):

$$A_e(x,\theta) = A_v(x,\theta) + \frac{\beta}{2q_\infty}\int_0^x L(x,\theta)\,dx \tag{1}$$

$$F(x) = \frac{1}{2\pi}\int_0^x \frac{A_e(\bar{x},\theta)}{\sqrt{\bar{x}-x}}\,dx \tag{2}$$

In the years following, several studies [21–23] validated the fundamental theory, and by the early 1960s, it was well established. It included arbitrary aircraft maneuvers, ray tracing through a horizontally stratified atmosphere with winds, and evolution of the far-field boom for an arbitrary F-function. The first and successful implementation of sonic boom fundamental theory was the Hayes, Haefeli, and Kulsrud code in 1969, known as the Hayes program or ARAP (Aeronautical Research Association of Princeton) program [24]. The program requires as input an F-function source and implements a ray-tracing formulation analytically derived from Fermat's principle. Whitham's rule is applied via the concept of signature aging, and shock coalescence is handled by numeric area balancing. ARAP made a major breakthrough in sonic boom research since it was the first code to apply the well-developed theory of geometrical optics to an acoustic problem. In 1972, Thomas [25] published a code that used a quite different algorithm for signature propagation. Thomas' program computes ray paths by direct numeric integration of the eikonal (by applying Huygen's principle) and applies Whitham's rule via the analytic waveform parameter method. A set of parameters is defined for a waveform complete description, and equations are obtained for the time rates of change of these parameters. Rather than beginning with an F-function, Thomas' program input is Δp longitudinal distribution at some radius. Whitham's and Thomas' methods are mathematically equivalent and give the same results since both represent the full implementation of fundamental theory, but the waveform parameter method appears to provide a more suitable approach for automatic computation [25,26]. In addition, Thomas' program provides the user with the possibility to directly input the pressure signature around the body from wind tunnel tests or CFD, instead of calculating it from the F-function. In fact, even if these two quantities are directly related, the actual Δp in the near-field does not necessarily correspond to the effective Δp from the F-function. This becomes significant especially when complex, low-boom-shaped configurations are analyzed. Both Hayes' and Thomas' programs are essentially single-point programs: one run of either yields the boom at a single azimuth and flight time.

This can cause stacked runs to be applied if a full mission analysis is required. These two programs are still actively used today, and represent a reference for what are termed full ray trace programs. Virtually every full ray trace sonic boom program is evolved in one way or another from one of them. One example is the first version of NASA PCBoom [27,28], which is an extension of Thomas code. Simplified implementations of fundamental theory are given instead in [29,30]: these are valid for analyses in a windless atmosphere. The first work by George and Plotkin [29] presented charts that allow the manual computation of signature evolution under the flight track. Carlson [30], on the other hand, developed a very useful handbook procedure for a "first-cut" estimation of far-field booms generated by steady flight in a standard atmosphere, where the ground signature is expected to be an N-wave. He provided equations similar to Whitham's far-field formulas but with several factors associated with propagation. These factors include the effect on amplitude and duration due to refracted ray paths and acoustic impedance gradients, and amplification due to reflection at the ground. Propagation off-track is included. The integral of the F-function is represented by a normalized shape factor scaled according to aircraft size [10]. Shape factors for several airplanes are given in a chart, and a simple procedure allows the calculation of it for types of aircraft not included in the chart. Refraction and impedance factors for flight in a standard atmosphere are contained in charts as well. With Carlson's method, an estimate of both overpressure and N-wave duration can be obtained. Carlson's method is valuable not only because it allows quick calculations of steady flight N-wave booms but also because it explicitly shows the scaling effect of parameters such as Mach number and aircraft length. Additionally, the shape factors can be used to generate effective F-functions to be used in full ray trace programs. This method is validated against numerical simulations (full CFD approach) in [31]. The agreement between the two methods occurs in the limits of validity of the N-wave model. Nevertheless, the Carlson method can be easily applied during the preliminary design of a supersonic aircraft with the purpose of selecting the baseline geometry on which to perform the optimization process through the CFD computations. A new empirical formulation to obtain useful predictions of the magnitude and footprint of the sonic boom that would be created by either known supersonic aircraft or new designs flying at a constant Mach number and altitude was developed in 2006 by Clare [32]. This research is based on the linear regression of independent parameter groups operating on the Lee and Downing 1991 database [33] of sonic booms created by military aircraft at Edwards Air Force Base, California, USA. The formulation employs an empirical F function that characterizes the near-field effects of shape, lift, and Mach number on the sonic boom. The prediction accuracy, as assessed by the scatter within the original database, is retained acceptably, and able to produce better correlations with respect to alternative analytical prediction models. However, the formulation can only make predictions of sonic booms generated by flying at a constant altitude and Mach number, and cannot make predictions for maneuvering aircraft. Summarizing, fundamental theory can provide accurate predictions of the sonic boom ground signature produced by supersonic aircraft, but some limitations arise from the assumptions on which it is founded.

Being the fundamental theory founded on linearized supersonic flow theory, it is valid just for slender bodies at moderate supersonic Mach numbers in inviscid and irrotational flow. Above Mach 3, in fact, slender-body theory does not provide reliable results [5]. Standard theory represents shock waves in the traditional gasdynamic form of zero-thickness pressure jumps. Real sonic boom shock waves have a finite rise time, occurring partly from turbulence and partly from molecular relaxation, which affects the high-frequency content of the boom spectrum. These frequencies are important for some human response loudness assessment techniques [34], and, for this reason, an artificial shock thickening method is required. Additionally, assumption of the N-wave signal at ground independently from the aircraft shape is made by Whitham [12]. In 1965, McLean showed for the first time that for a representative supersonic aircraft, the signature would not actually reach the asymptotic state at ground until much further than a cruise altitude of 44,000 feet [35], and the distances at which far-field is reached depend on the shape of the aircraft. Furthermore,

in real atmospheric conditions, characteristics coalesce more slowly than in uniform atmosphere, increasing the possibility that non-fully coalesced N-wave signatures shapes may reach the ground. In the end, turbulence, as well as atmosphere variability and absorption effects, are not accounted for in pressure signature propagation. In particular, turbulence modeling, although difficult, results to be of particular interest as to whether the waveform distortion caused by its presence will adversely affect the loudness of minimized sonic boom signatures associated with low-boom supersonic transport. The fundamentals of sonic boom theory were established and validated in the 1950s and early 1960s, and since then, there has been significant research and advances in both the understanding and modeling of sonic boom. The substantial growth in computing power and its widespread availability have allowed for the development and use of more sophisticated prediction methods and tools. These include full CFD solutions for the near-field pressure signature computation, and the iterative resolution of the augmented Burgers' equations for signature propagation to the ground. Turbulence and nonstandard atmosphere effects could even be modeled and included.

2.1.2. Advances in Near-Field Prediction

Near-field pressure signature prediction according to Whitham's theory provides that the effect of geometry and lift must be modeled with an equivalent axisymmetric body of revolution, and as the complexity of the geometry increases, this process becomes difficult [36]. A solution to that is given by using Euler CFD solutions to obtain the near-field pressure signature [37–40]. CFD makes it possible to treat a model of real aircraft geometry without any simplification or transformation. Moreover, by running viscous as opposed to inviscid simulations, more accurate pressure information can be extracted, and plume effects [41], as well as inlet integration [42] can be taken into account. The complexities associated with such a numerical method mainly relate to the fact that a careful grid generation is needed to properly define the computational domain, and solutions become increasingly more expensive as the domain size increases. An obvious approach to using CFD would be to extend the domain and carry the calculations out to distances, where a far-field condition is met. However, for complex configurations, such as low-boom supersonic transports, this condition may not be met, even at distances of five or ten body lengths [38]. The cost, in terms of both computational power and time, is high, especially when the domain must be extended out far enough so as to correctly match the three-dimensional CFD solution with the one-dimensional propagation models (or to convert CFD pressure signals into equivalent far-field radiating source distributions [10]). Although some techniques have been developed to match the three-dimensional near-field solution provided by CFD with the propagation codes [37,43–45], by allowing for a smaller domain to be used for the near-field solution, as computational technology has continued to grow rapidly and solutions methods have improved, it has become common to increase the domain size enough to provide a pressure signature that is well approximated as one dimensional. This still comes at a high computational cost. As a result, CFD solutions are not suitable for applications such as trade-off studies or optimizations that involve a big number of configurations to analyze, typically carried out during conceptual and preliminary aircraft design stages. On the other hand, high-fidelity methods are the only available solution for detailed design and/or multi-disciplinary optimization studies. A reasonable trade-off consists in implementing CFD solutions to build response surfaces or surrogate models. Another option to obtain the near-field pressure signature around almost any complex geometry with a computational cost that is orders of magnitude smaller than a full CFD solution is to use 3D high-order panel methods [46–48]. These methods, developed heavily in the 1970s and 1980s, can provide a linearized inviscid supersonic solution of the near-field flow around the aircraft and have been used in optimization studies of low-boom configurations [49–51]. Even with panel methods, the geometry is modeled directly. Consequently, three-dimensional effects, such as lift and shielding effects, are determined without the need of generating equivalent axisymmetric bodies as in classical

theory. However, since they provide a linearized inviscid solution, their use is restricted to slender bodies at low Mach numbers. Unlike full CFD, panel methods can provide a near-field solution at any distance away from the aircraft without additional computational costs. However, since this solution is linear and assuming a uniform flow field, the error increases with distance. Chan [49] proposed a methodology for correcting the error due to the linearity of the panel solution. It involves calculating the near-field signature by using a panel method, finding an equivalent axisymmetric source distribution, and then using the fundamental theory. This takes into account the nonlinearity, to calculate a new near-field corrected signature. According to Giblette [46], panel methods for near-field pressure signature prediction give results that are in good agreement with CFD for a simple axisymmetric geometry, while comparisons made on more complex geometries highlight the shortcoming of using a potential flow solution, in which unrealistically large velocities are calculated on sharp corners (in the case of a wing-body configuration, i.e., it could happen at the wing tip and on the side of the fuselage tail). Panel solutions show local large spikes in the signature that do not exist in the CFD signature, and that results in local large differences in both the ground signature and perceived loudness. Another solution could be the revisited version of the fundamental theory presented in [36]. Whitham's F-function is substituted by a modified Lighthill F-function to generate the near-field pressure signature. The derivation of Lighthill's F-function does not require the assumption of a smooth area profile as in the case of Whitham's F-functions. This is a significant improvement, which allows Lighthill's F-function to be applied to objects that have discontinuities. The study demonstrates that the modified Lighthill method is able to predict the sonic boom shape, magnitude, and duration within 10% with respect to pressure profiles from wind tunnel experiments, computational fluid dynamics, and flight tests, and account for variations in lift, Mach number, and propagation angle. However, in general, modified linear theory is capable of producing a first-order pressure profile, as long as the aircraft model can be resolved into an axisymmetric area profile. With run times less than a minute, and considering that no mesh generation is required, it is appropriate for the preliminary and conceptual design stages of quiet sonic boom aircraft. Summing up, the modified Lighthill function and panel methods represent a good approach for design space exploration or preliminary optimization studies of low-boom aircraft configurations, where large numbers of basic geometries are analyzed and approximate results are sufficient. These methods can also be used to generate surrogate models, even together with high-fidelity level ones [48] in a multi-fidelity framework.

2.1.3. Advances in Pressure Propagation

As in the case of near-field solutions, new methods and models have been developed even for the propagation of signatures to the ground. They try to overcome the limitations inherited with the application of fundamental theory. In particular, fundamental theory is not able to predict the shock rise time since weak shock theory assumption is made. The predicted ground signatures using traditional approaches present the shocks as discontinuous jumps, and during the calculation of the frequency spectrum and successive noise metrics, empirical or numerical shock thickening, as well as the shock-merging procedure, must be taken in place to correct or adjust the signature. This is essential because Fast Fourier Transform (FFT) and other numerical techniques required in computation of any noise or loudness metric cannot be applied to a waveform with discontinuities. However, the shock-thickening and -merging processes are subject to errors since rise times calculated are heavily dependent on the empirical or numerical factors chosen for converting the discontinuous shocks into continuous profiles, and may produce loudness or other noise metrics that are not accurate [52]. This becomes a problem especially during optimization studies, where the optimizer could exploit the shock-merging process to its advantage. Several research studies have looked at boom prediction methods that compute the rise times, instead of empirically adjusting or correcting the ground signature, resorting to weak shock theory and area balancing. The most used method is to account for molecu-

lar relaxation (a dominant mechanism in sound absorption for the frequencies typically associated with sonic booms (e.g., 1–100 Hz), responsible for thickening the shocks), absorption, atmospheric stratification and spreading terms in the governing equation, called the augmented Burgers equation [52–55]. Augmented Burgers equations differentiate from regular equations that just account for the nonlinear term. Burgers' equation describes the evolution of the acoustic field along a ray-theoretic propagation path [56]. The classic way to solve the augmented Burger equation is by means of the operator-splitting method [50]. In 2015, Yamamoto et al. [57] proposed a different approach ("Burgers-Relax-Uni") to solve the augmented Burger equation. An internal variable is introduced, which can be solved analytically at each step. As a result, the decomposed equations with the internal variable can be solved as a system of equations by being lumped into a matrix form. This algorithm demonstrated to be almost twice as fast as the original method and more stable. It can suppress the numerical oscillation of propagating boom at high altitude. Furthermore, different algorithms exist to handle propagation mechanisms. Some methods, like the one presented by Pilon [55] or the one developed by Robinson [54] and implemented in ZEPHYRUS code, uses the frequency domain to account for the dissipation and relaxation. Others methods, like the one from Cleveland [53], successively extended by Rallabhandi [52] in sBOOM, implements a time domain algorithm to account for all the propagation mechanisms.

Frequent conversion from the time domain to frequency domain and back during atmospheric propagation may lead to numerical errors. Even if these can be bounded, frequent FFT and inverse FFT operations add an additional computational load during the propagation process. The most relevant limitation connected with codes that solve the augmented Burgers equation is the longer computation time needed for calculating the sonic boom footprints, with respect to the ones which implement the fundamental theory. On average, the time to run such a codes is about 20–25 times slower than linear codes [52].

Another advanced propagation method is developed by solving a Full Potential Equation (FPE) to the ground [58]. This three-dimensional CFD method can march the solution with atmospheric changes in pressure and temperature taken into account. The nonlinearity and nonaxisymmetry of the Full Potential propagation code makes it superior with respect to the other prediction methods that implement the linear ray-tracing approach. However, it needs better validation against numerical and experimental measurements. Advances have also been made in the modeling and prediction of other atmospheric phenomena that could affect the sonic boom waveform at the ground, and, as a consequence, their loudness and annoyance levels. One important phenomenon having a great impact on sonic boom is turbulence. The effect of atmospheric turbulence on a sonic boom can be interpreted as a smoothing deformation of the wavefront due to both velocity and temperature turbulent fluctuations in the medium through which it propagates. In particular, there is a ragged fine structure behind each shock, and the shock rise times tend to be longer and variable [10] (Figure 3). The essence of the effect of atmospheric turbulence on sonic boom waveforms is the scattering of acoustical waves and a series of focused/defocused wavefronts.

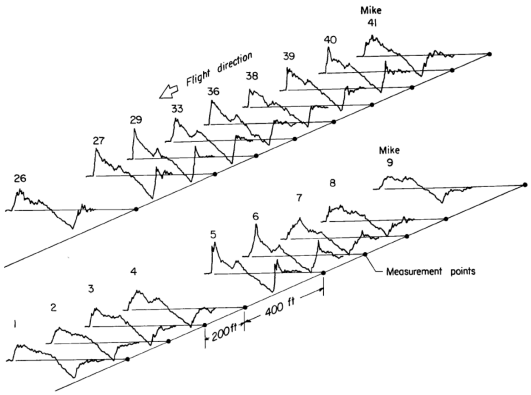

Figure 3. Sonic booms measured under calm and turbulent atmospheric conditions [59].

The effect of atmospheric turbulence on sonic booms has been investigated theoretically, experimentally, and numerically. Crow [60] first explained the fine structure by scattering theory and estimated the order of the rise time due to atmospheric turbulence from his insightful theory based on a statistical approach. Based on Crow's estimation, Pierce [61], Pierce and Maglieri [62], and Plotkin and George [63] independently developed more detailed estimations of rise time and considered the means by which atmospheric turbulence lengthened it. Turbulence that affects sonic boom signature propagation is known as the planetary or Atmospheric Boundary Layer (ABL) because it is limited to propagation from altitudes up to 6 km. The ABL varies daily and should be modeled as both random temperature and velocity fluctuations fields. Therefore, turbulence effects are predicted by calculating sonic boom propagation through an ABL model. In order to propagate sonic boom pressure signatures accounting for turbulence distortions, the augmented Burgers equation alone is not sufficient. Useful results have been obtained by using the Khoklov–Zabolotskaya–Kuznetsov (KZK) equation as a propagation equation [59,64,65]. Turbulence model research codes based on this equation solution have been developed within the Sonic Booms in Atmospheric Turbulence (SonicBAT) Program by NASA and incorporated into the PCBoom sonic boom prediction software to estimate the effect of turbulence on the levels of shaped sonic booms associated with several low boom aircraft designs [66]. Other nonlinear models have also been applied to sonic boom propagation, including a a time domain solution of the nonlinear progressive wave equation (NPE) [67], a combined time domain and spectral approach called FLHOWARD [68] using a partially one-way equation and a similar but one-way equation called HOWARD [69,70]. The latest methodology has been implemented in a code developed in 2021 called SPnoise for Sonic Boom [71]. KZK implementation assumes what is termed the parabolic approximation, including the assumption that propagation is primarily in one direction but is better-behaved at domain boundaries than the NPE solution and the computation does not require the FFTs used in FLHOWARD or HOWARD. On the other hand, the solution of KZK may be sufficient if the solution of interest is close to the sound axis, but when the scattering is widely distributed, it results in an unsatisfied description of distorted signatures [71]. An atmospheric turbulence model is also needed in conjunction with a propagation equation to simulate a random turbulent field throughout the domain. Turbulence is represented as both temperature and wind fluctuations, usually taken from measurements or inferred. In [72], the great influence of atmospheric turbulence parameters on both classic N-waves (on which turbulence has greater influence) and low boom pressure signatures at the ground is shown, highlighting the need of stochastic studies. Another important phenomenon that needs to be carefully predicted and simulated is focused booms. Focused booms develop during supersonic aircraft accelerations in climbing, turning and maneuvering (Figure 4): although most focus booms can be avoided or minimized, the transition focus during acceleration from subsonic to supersonic speeds is unavoidable. Hence, its evaluation becomes fundamental for future low-boom aircraft in order to assess the acceptability of overland supersonic flight. Focused boom, also known as 'sonic superboom' leads to the amplification of ground pressures up to two or three times the carpet boom shock strength [73]. The focusing of shock waves occurs at surfaces called caustics. Caustics are surfaces where the ray tube area vanishes and geometrical acoustics becomes singular, predicting infinite overpressures. Factors which are neglected in the development of geometrical acoustics become important at focal points and serve to limit pressures to finite values. Substantial research on the behavior of a sonic boom at focus has been conducted over the past decades. The equation that describes the sonic boom pressure signature near the caustic is the nonlinear Tricomi equation, which includes diffraction effects neglected in standard sonic boom theory, as well as the usual first-order nonlinear term. Both of these limit the amplitude of the focused booms. The diffraction limit is frequency-dependent, affecting low frequencies more than high frequencies, leading to a characteristic U-wave shape with the shocks peaked (Figure 4).

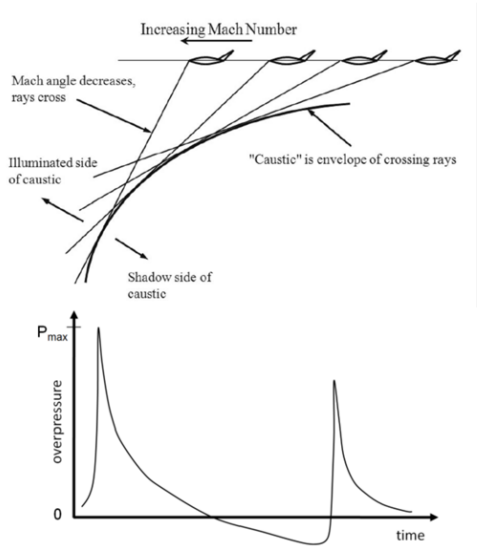

Figure 4. Caustic due to acceleration (**up**) and typical focused U-wave sonic boom (**down**) [74,75].

In 1965, Guiraud [76] wrote the equations for the focus of weak shock waves and developed a scaling law, while Seebass [77] found a way to linearize the Tricomi equation through a Legendre transformation. If no shock is present near the caustic, his transformation effectively linearizes the problem. Gill and Seebass [78] obtained a numerical solution for the focus of a step function at a caustic. Using Guiraud's scaling law, Plotkin and Cantril [79] extended PCBoom to apply Gill and Seebass' solution at focal zones. That code has evolved into PCBoom3 [10]. Marchiano and Coulouvrat [80] re-derived Guirads' formulation of the nonlinear Tricomi equation, while Auger and Coulouvrat [81] presented an algorithm to solve the nonconservative, nonlinear Tricomi equation by using a Fast Fourier Transform. Kandil and Zheng [82,83] presented a different approach by splitting the Tricomi equations into the linear unsteady Tricomi equation and the nonlinear unsteady Burgers equation. Three computational schemes were developed: a frequency domain Fast Fourier Transform scheme, a time domain finite difference scheme and a time domain finite difference with overlapping grid (OLG) scheme. Piacsek in [84,85] instead used the nonlinear progressive wave equation (NPE) as a prediction method for focused booms. A study conducted at NASA in 2012 [86] aimed at comparing different prediction methods with flight test field measurements, showed that the Gill–Seebass method tends to overpredict local peaks, and thus, it is not applicable to complex signatures. In contrast, the NTE method with absorption appears to be better suited to the prediction of complex signatures, such as low-boom shaped signatures. Methods resulting from these studies have been implemented in sonic boom propagation codes. Aside from PCBoom3, TRAPS [87] accounts for the passage of a boom through caustics via a Hilbert transform. It is successful in predicting where focusing reaches the ground, but it gives excessively large amplitudes. ZEPHYRUS [54] tends to resolve the discrepancy of TRAPS by incorporating the air absorption effects. It predicts lower values for the overpressure as compared to TRAPS but is much more computationally intensive. In 2017, Rallabhandi [88] developed a way to numerically predict focused sonic boom signatures using both Gill–Seebass similitude and the solution to the non-linear Tricomi equation to be included in sBOOM.

2.2. Loudness and Annoyance Metrics

When an analysis of sonic boom caused by a supersonic aircraft is carried out, not only is the prediction of the phenomenon important but also the quantification of the annoyance caused to people (outdoor and indoor), the magnitude of structure vibrations and the measure of secondary effects, such as rattle. In this regard, the selection of metrics able to reflect sonic boom effects is one important step in evaluating the potential impact

of introducing civil supersonic flight overland. However, still today, a unique acoustic measure to define boom acceptability levels is not established yet. Important research centers, like NASA and JAXA, have conducted several surveys, laboratory studies and low-boom flight tests to identify the correlation between metrics and sonic boom, with the aim to support and help ICAO in developing new certification standards. The European project RUMBLE (RegUlation and norM for low sonic Boom LEvels) [89] also plays a role in this regard. The project is, in fact, dedicated to the production of the scientific evidence requested by national, European and international regulation authorities to determine the acceptable level of overland sonic booms and the appropriate ways to comply with it. The main actions of the project are the development and assessment of sonic boom prediction tools, study of the human response to a sonic boom, and validation of the findings using wind tunnel experiments and actual flight tests.

Different metrics could be retained as an objective for sonic boom reduction and minimization. They can be categorized as pressure based or loudness based. To the first category belongs the maximum peak overpressure, front shock overpressure, sum of the shock amplitudes, while Sound Exposure Level (SEL), A-weighted Sound Exposure Level (A-SEL), C-weighted Sound Exposure Level (C-SEL) and Perceived Loudness deciBel (PLdB) belong to the second one. Pressure-based metrics are the most used in optimization problems, but they do not provide a cost function that synthesizes at the same time the energy content and the full frequency of the signature. Loudness metrics, instead, result from the mathematical process of the signal: it causes the loss of direct dependencies between the geometry (the input of the problem) and the metrics (the output of the mathematical system), but, on the other hand, brings the energy and frequency content of the signal that has a direct impact on the annoyance evaluation. It is clear that the choice of such an objective function is not a trivial process and results from a compromise between the accurate description of the physical phenomenon and correlation between the function itself and the design variables.

In [90], loudness and short-term annoyance ratings were collected for conventional and low-boom signatures at low overall levels. The average annoyance ratings were best reflected by ASEL (A-weighted Sound Exposure Level) values compared to other frequency weightings. Moreover, the results of the listening experiments showed that the tested low-boom designs are similarly loud and annoying as conventional and N-wave sounds when presented at similar ASEL values, and an indication of a systematic benefit for low-boom signals compared to conventional booms was not observed. However, other studies [91–93] indicate that psycho-acoustic loudness models or the inclusion of a loudness derivative and duration for the description of the sound character in multi-metric annoyance models can enable a better characterization of the perception of transient sounds than single level-based measures. Metrics including time-varying loudness models, such as those developed by Glasberg and Moore [94] or Zwicker and Fastl [95], may be useful for predicting the impact of impulsive sounds since they incorporate models of the temporal behavior of the human hearing system, which is clearly of importance with rapidly changing sounds. The output from their models is a profile of the loudness heard through time as opposed to a single number representing the whole or part of a sound event. Moreover, it has been noted [96] that sonic boom pressure signatures measured using microphones on the ground are different at different locations, even though nothing about the aircraft or its speed has changed. This is due to the turbulence effect, and makes it even harder to define a standard method of measurement and evaluation. An attempt to find metrics more stable to turbulence was made in [97]. According to this work, B-SEL could be a good candidate for certifying supersonic aircraft for overland civil transportation.

Another relevant topic is the difference between indoor and outdoor sonic boom effect. In 1993 [98], the sonic boom simulator of the Langley Research Center was used to quantify subjective loudness and annoyance response to simulated indoor and outdoor sonic boom signatures. Two indoor listening situations were simulated: one with the windows open and the other with the windows closed. The results were used to assess loudness and annoyance as sonic boom criterion measures and to evaluate several metrics. The findings

indicated that loudness and annoyance were equivalent criterion measures for outdoor booms but not for indoor booms. Annoyance scores for indoor booms were significantly higher than indoor loudness scores. Thus, annoyance was recommended as the criterion measure of choice for general use in assessing sonic boom response. Perceived Level [99] was determined to be the best estimator of annoyance for both indoor and outdoor booms, and of loudness for outdoor booms.

The Okhlahoma city survey [100] showed that the best correlation with the annoyance is achieved using the number of boom per day. The survey recommends a boom peak pressure level of $35.91/\sqrt{N}$, where N is the number of boom per day.

When it comes to the evaluation of sonic boom indoor perception, not just the audible component of the signal should be considered. Tactile motion of the building, as well as rattling (occurring for structural elements not well mounted or constrained) of the building and of the objects inside the building must be taken into account, and the last two require the introduction of a dynamic model of the structure. The simplest approximation is the lumped parameter single degree of freedom model [101] but is obviously a limitation. The wall dynamic behavior is, in fact, always coupled to the interior, and a multimodal analysis is required [102].

Figure 5 provides a summary of the main metrics suggested to be adopted as more representative of the sonic boom effect, and can be used for optimization problems, along with reference values.

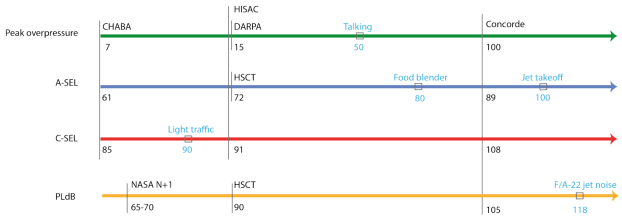

Figure 5. Sonic boom metrics proposed compared to reference values linked to ordinary events [103].

2.3. Minimization Theory and Techniques

Sonic boom minimization became of great interest during the 1960s and 1970s, when knowledge of the phenomenon's physics and its calculation and prediction was already assessed. The first theoretical approach used as a key point was Whitham's F-function since it constitutes the link between the aircraft configuration and the pressure signature. Jones [104] and Carlson [105] were the first to suggest that a reduction in the sonic boom could have been achieved by aircraft shaping. Based on the assumption that all pressure signatures reaching the ground would have the characteristic N-wave form, they defined an equivalent-body shape, which can produce an N-wave signature with a "lower bounded" over pressure and impulse. The area distribution they ended up with was extremely blunt, and the shape changes required to produce such equivalent areas resulted in being detrimental in terms of drag [106]. Later, in 1965, McLean found that during transonic acceleration, the signature created by large and slender SSTs might not necessarily attain their far-field N-wave form, and Hayes pointed out that in the real atmosphere, characteristics coalesce more slowly by making it possible to "freeze" the shape of the midfield signature and keep it until the ground [107]. Since the shape of a midfield signature strongly depends on the shape of the aircraft, such shaping was recognized as a much more powerful way of minimizing the boom.

George and Seebass [108,109] developed a relatively complete theory, in which they found the lower bounds for the bow and the tail shock of a midfield signature. It laid the theoretical foundation for the sonic boom minimization method. However, the nose shape determined by the minimized area distribution was as blunt as in the previous theories, with the consequence of a significant drag penalty. The low boom–high drag paradox is shown in a scheme in Figure 6. In addition, this method sacrificed the front fuselage size, resulting even in the reduction in usable fuselage space. Darden, in 1979 [110], advanced

the George and Seebass' method by controlling the bluntness of the area distribution near the nose, overcoming the drag rise problems associated with the previous theory.

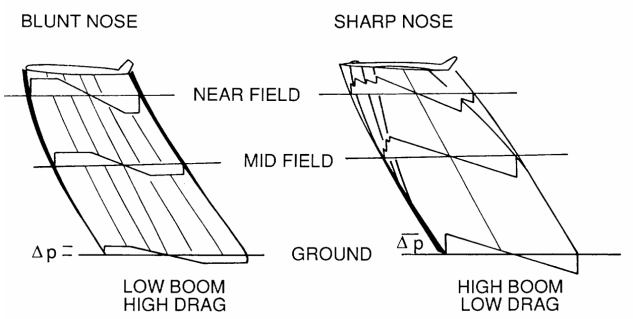

Figure 6. Low boom–high drag paradox (Source: [107]).

The final theory is known as Seebass–George–Darden, SGD, theory. It states that, given the flight conditions of altitude and Mach number and the aircraft parameters of weight and length, the equivalent area distribution needed to create either a minimum overpressure signature or a minimum shock signature can be defined. Carlson and Mack [111,112] applied the minimization method to several conceptual aircraft and ran a wind-tunnel test program to validate it. The Shaped Sonic Boom Demonstration (SSBD) program successfully tested the low-boom theory to be reliable under actual flight and atmospheric conditions.

Lately, Mack [113], Rallabhandi [114] and Plotkin [115] extended and generalized the SGD theory, by making it more flexible with respect to the trade-off between boom minimization and other performance measures, and more suitable for practical design. They also provided lower bounds for the perceived loudness.

The SGD sonic boom minimization process produces cross-sectional area profiles that generate either a minimum overpressure "flat-top" signature (Figure 7b) or a maximum-rise-time boom, which has a small initial shock pressure rise (ISPR) followed by a gradual increase to the peak overpressure (Figure 7c). These sonic boom types are essentially modified N-waves. Another option to reduce the annoyance of the sonic boom to humans is to generate a multishock signature (Figure 7d) by means of a lobe-balancing method [116,117]. Lobes are created using lift, by trimming lifting surfaces to obtain a frozen, shock balanced F-function, like the one showed in Figure 8, at different flight conditions.

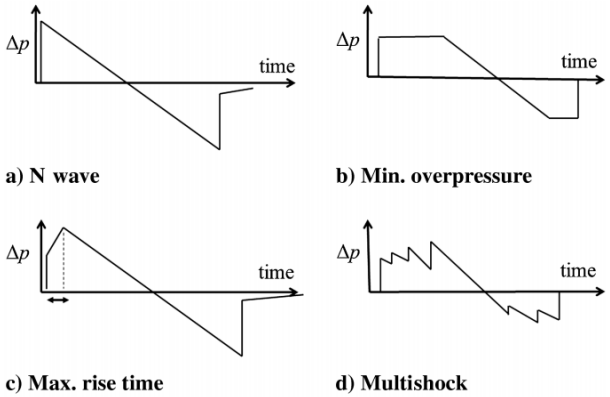

Figure 7. Types of sonic boom signatures (Reprinted/adapted with permission from Ref. [116], copyright 2023, Jung, T.).

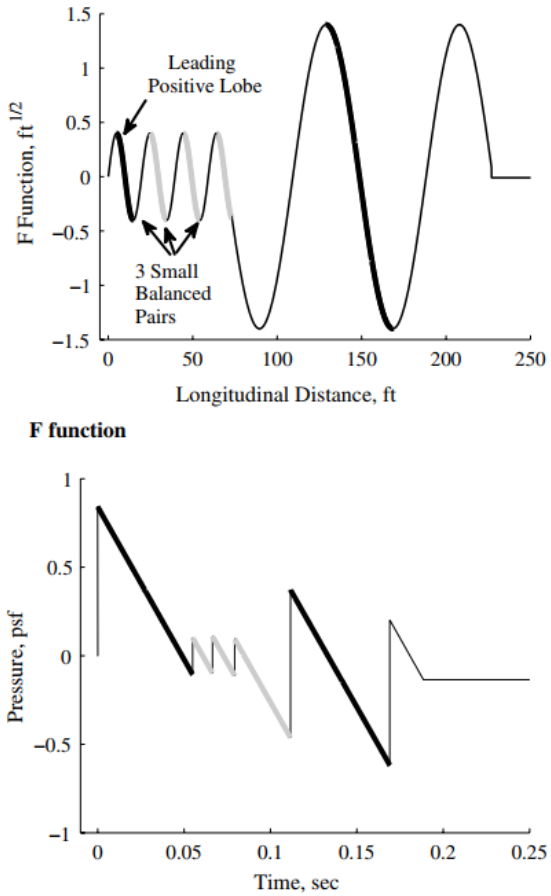

Figure 8. Example of a lobe-balanced F-function and corresponding ground pressure profile (Reprinted/adapted with permission from Ref. [116], copyright 2023, Jung, T.).

Sonic boom minimization techniques through aircraft shaping are implemented still today through the inverse design approaches for optimization and low-boom design problems. The inverse design approaches have been widely adopted [118–121]: a target near-field or far-field pressure signature is designated by means of minimization techniques, and achieved by aircraft shape optimization. Different optimization methods and algorithms are used, such as the CFD adjoint-based and genetic algorithm. Zhang [122] used instead the Proper Orthogonal Decomposition (POD) method to develop an inverse design framework for supersonic low-boom configuration. In the end, in a recent work [123], the low-boom design challenge was resolved by using reversed equivalent area targets for low-fidelity low-boom inverse design and a block coordinate optimization (BCO) method for multidisciplinary design optimization (MDO). The corresponding low-boom MDO problem includes aircraft mission constraints on ranges, cruise speeds, trim for low-boom cruise, static margins for take-off/cruise/landing, take-off/landing field lengths, approach velocity, and tail rotation angles for trim at take-off/landing, as well as fuselage volume constraints for passengers and main gear storage. The BCO method was developed to optimally resolve the conflicts between the low-boom inverse design objective and other design constraints.

2.4. Critical Review

In this section, all the methods for the prediction of sonic boom are presented, from the fundamental Whitham F-function and the simplified Carlson method, up to the most advanced methods for both near-field pressure distribution and pressure propagation calculation. Figure 9 provides a summary of the different methods with their strengths and limitations.

Method	Strengths	Limitations	Applicability
Carlson	Provides a fast and good estimation of sonic boom at the ground by means of semi empirical equations and charts	Assumes N wave signal at the ground Valid only for conventional military and civil configurations	Conceptual Design Phase
Witham's F-function	Analytical method based on linearized supersonic flow theory and geometrical acoustics method for propagation Easy implementation for computational analysis	Based on linearized supersonic flow Not applicable to non slender configurations and at high mach numbers	Conceptual Preliminary Design Phase
3D Panel Method+ Propagation code	3D Geometry modelled directly (no equivalent axysymmetric body needed as in Whitam's F-function) Computational cost is very low (run time of about seconds)	Not applicable to non slender configurations and at high mach numbers	Conceptual Design Phase
CFD+Propagation code	Physical based solution, valid for any aircraft configuration. Accurate prediction of shocks strength and location (mesh accuracy becomes fundamental	Computational cost is high and increase with distance form the body (run time from minutes to hours)	Preliminary Design Phase
Full CFD solution	Very accurate solution at the ground. Shocks coalescense trhough propation in the atmosphere physically simulated, real boom signature shape at the ground Focused sonic boom phenomena can be treated	Computational cost is very high and demanding (run time hours or days)	Detailed Design Phase

Figure 9. Review of sonic boom prediction methods.

Section 2.3, instead, provides an overview of the minimization techniques, developed over the years to shape the signal at the ground by optimally shaping the airframe. Sonic boom minimization is based on the Seebass–George–Darden (SGD) theory. According to this theory, given the flight conditions of altitude and Mach number and the aircraft parameters of weight and length, the equivalent area distribution needed to create either a minimum overpressure signature or a minimum shock signature can be mathematically defined. From the equivalent area distribution, the optimal aircraft shape can be easily found. The Shaped Sonic Boom Demonstration (SSBD) program successfully tested the low boom theory to be reliable under actual flight and atmospheric conditions. Further studies on this theory led to another technique to reduce the annoyance of the sonic boom on humans: the lobe-balancing technique. By trimming the lifting surfaces, a frozen shock balanced F-function could be generated, resulting in a less annoying multishock signature at the ground. These two minimization techniques have been used in several inverse design and optimization processes, where a target near-field or far-field pressure signature is achieved by careful aircraft shaping. Different optimization methods and algorithms can be used, such as the CFD adjoint-based and genetic algorithm.

However, though shaping the aircraft to reach the minimum sonic boom could effectively end in a low-boom aircraft configuration, it could lead to unfeasible solutions, especially in terms of cabin volume. In addition, the curved shaped body would strongly perturb the air stream flowing around the aircraft, affecting also aerodynamics. In the end, as already highlighted in the section, the low-boom requirements are in conflict with the low-drag requirements. A trade-off between these two fundamental requirements must be found in the next generation of supersonic aircraft, and this leads to not consider sonic boom minimization theories and techniques as a good solution.

3. Sonic Boom Reduction

3.1. Aircraft Operations

The sonic boom produced by aircraft in supersonic flight is attributed mainly to both its volume and the lift it generates: it implies that size and weight play a major role in establishing the intensity of the signal at the ground. Moreover, since the boom at the ground is a direct consequence of the shock propagation from the cruising altitude, the latter has a fundamental impact on it. Figure 10 shows that as the altitude increase, the total overpressure decreases significantly. As a result, flying higher could alleviate the sonic boom effect at the ground without changing the design of the aircraft.

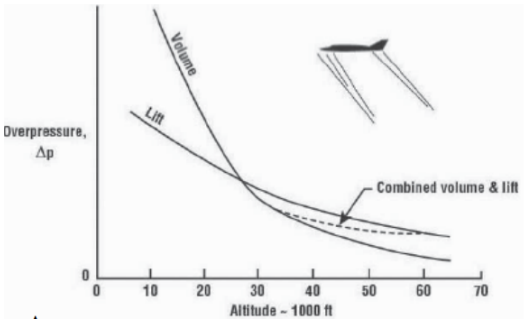

Figure 10. Altitude effect on overpressure due to both lift and volume (Source: [124]).

However, it is interesting to note that when the cruising altitude is increased to reduce overpressure through attenuation, the local speed of sound starts to decrease (due to decreasing density), making the aircraft fly at a higher Mach number relative to the local speed of sound, leading to a louder boom as depicted in the graph in Figure 11.

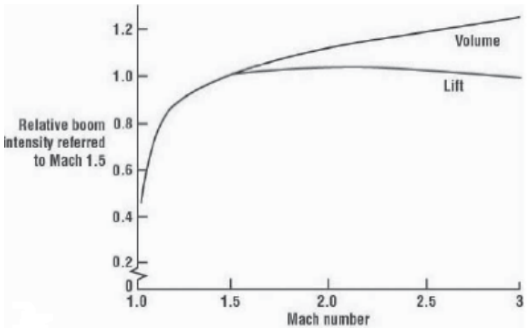

Figure 11. Speed effect on overpressure due to both lift and volume (Source: [124]).

Moreover, flying higher could lead to higher NOx emissions and fuel consumption.

Another way of reducing the sonic boom at the ground by flight operations is to fly at or below the so-named cut-off Mach number. Taking advantage of the temperature gradient of the atmosphere to refract the sonic rays upward [125], the sonic boom never reaches the ground. The Mach cut-off phenomenon is independent of the aircraft configuration and allows boomless flight up to a local Mach number of 1.15 in an ideal, standard atmosphere [126].

The Mach cut-off is seen by some manufacturers, such as Aerion, as a relatively low-risk way to operate a first-generation civil supersonic aircraft overland. It offers an approximately 23%, speed advantage over subsonic aircraft operating at transonic speeds, and at the same time, it avoids the many risks of low-boom designs [127]. The FAA recently funded Mach cut-off research through the ASCENT Center of Excellence. NASA also recently studied Mach cut-off and evanescent waves as part of the Farfield Investigation of No-boom Thresholds (FaINT) program [128] and in the Low Boom/No Boom flight test [129].

3.2. Aircraft Configurations for Low Boom

3.2.1. Current Promising Concepts

Reducing the sonic boom to acceptable levels for enabling supersonic flights overland is a very hard and challenging objective, and for this reason, the exploration of new disruptive unconventional technologies and configurations is needed. The most promising steps taken in recent years, along with ongoing projects and programs in this regard, are here presented and described.

The DARPA Quiet Supersonic Platform program [130], started in 2000, is directed towards the development and validation of critical technology for long-range advanced supersonic aircraft with substantially reduced sonic boom, reduced takeoff and landing

noise, and increased efficiency relative to current technology supersonic aircraft [131]. The target of this program was a 100,000 lb class vehicle with 20% pay load mass fraction. The resulted concept demonstrated to achieve the low sonic boom requirement, and a large majority of the goals is shown in Figure 12.

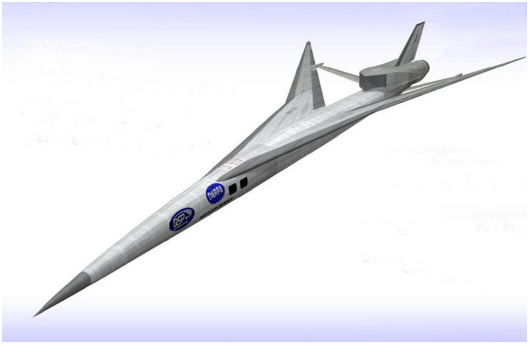

Figure 12. Concept of a quiet supersonic aircraft designed for both civil and military purposes. (Source: [132]).

The Shaped Sonic Boom Demonstration (SSBD) (2001–2003) was a two-year program led by Northrop Grumman Corporation, and including DARPA and NASA, which used a Northrop F-5E with a modified fuselage (Figure 13a) to demonstrate for the first time in flight that the aircraft's shock wave, and accompanying sonic boom, can be shaped, and thereby reduced. The program became, at that time, the most extensive study on the sonic boom. The SSBD demonstrated a reduction in boom by about one third. NASA continued to explore new aircraft designs capable of reducing the noise level of sonic booms by test flying an F-15B modified with an extendable boom (Gulfstream Quite Spike) on its nose (Figure 13b). It was part of the Gulfstream Supersonic Technology Program aimed at conducting basic research into reducing the impact of sonic booms on people and the environment to enable regulatory change for supersonic flight overland, domestically and internationally. The combined effort of NASA and Gulfstream resulted in an experimental plane concept initiated in 2008, the X-54 (Figure 13c). X-54 intended to continue the research objectives of the DARPA Quiet Supersonic Aircraft, and to demonstrate low-boom technologies and methods validated by projects such as the Quietspike project [133], the Shaped Sonic Boom Demonstrator [134], FaINT Project [135], and WSPR Project [136]. The X-54 will be designed from the ground up to incorporate all the technology and lessons learned from this combined NASA research spanning several decades into a viable aircraft capable of producing under 75 pdB on the ground while cruising over Mach 1.4 above 50,000 ft [137]. Its most notable features include a nose spike device for sonic boom reduction and a swing-wing configuration to balance supersonic cruise and low-speed performance.

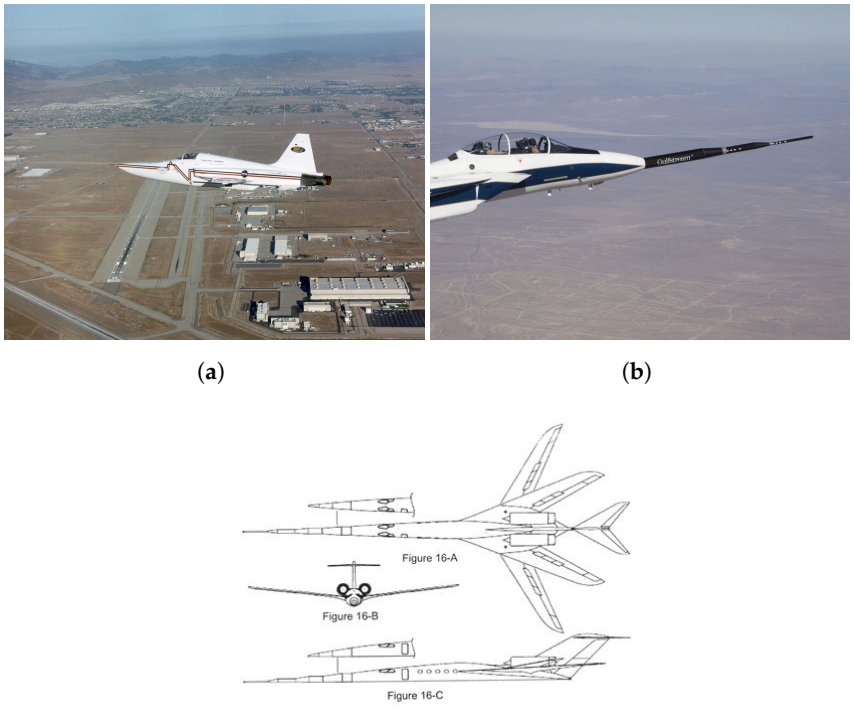

(**a**) (**b**)

(**c**)

Figure 13. NASA F5-E (**a**) (Source: [134]), NASA F15 equipped with Gulfstream Nose Spike (**b**) (Source: [138]) and NASA-Gulfstream X-54 experimental aircraft concept drawing (**c**) (Source: [139]).

The JAXA D-SEND (Drop test for Simplified Evaluation of Non-symmetrically Distributed sonic boom) project (2010–2015) ran flight experiments to demonstrate the possibility of a "low-sonic boom design concept" and to acquire measurement methods for aerial sonic booms, contributing to the ongoing deliberation of international standards for sonic booms of next-generation supersonic aircraft. The project comprised two phases: through D-SEND#1, JAXA established, for the first time, a new method of demonstrating the low sonic boom design concept and sonic boom measurement system in the form of a balloon drop test, while during D-SEND#2, an experimental supersonic glider model called the "Silent SuperSonic Concept Model (S3CM, S-cube Concept Model)", designed to reduce sonic booms originating from the front and rear, was flown at supersonic speed. They also ran evaluation tests using sonic boom simulators to assess how humans sense them and how buildings are affected [140]. In the end, JAXA cooperated with the SKY Aerospace Institute on a SSBJ design (Figure 14) [141]. The main features are the cranked arrow wing that uses natural laminar flow technology and a non-symmetrical fuselage to mitigate sonic booms. All these technological achievements come from these several projects JAXA has been involved in for years.

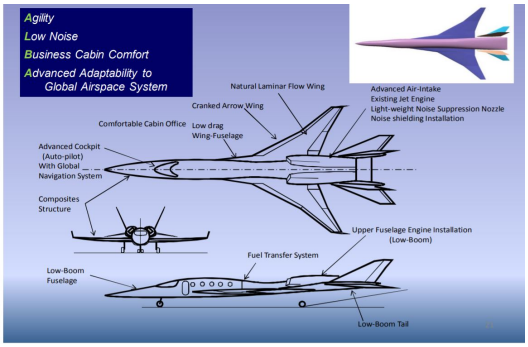

Figure 14. JAXA and SKY Aerospace business jet concept (Source: [142]).

The main objective of HISAC (environmentally friendly HIgh Speed AirCraft) European project (2005–2009) was to establish the technical feasibility of an environmentally compliant supersonic transport aircraft through an MDO approach and focused technological improvements. As a result, HISAC provided achievable specifications for an environmentally compliant and economically viable small-sized supersonic transport aircraft and recommendations for future supersonic environmental regulations (community noise, emissions, and sonic booms), enabling technologies and a road map for their further maturation and validation [143]. Three optimized aircraft configurations came out for low noise, long range and low boom (Figure 15).

Figure 15. HISAC project concepts for low noise (**left**), long range (**center**) and low boom (**right**). (Source: [144].)

The SENECA ((LTO) noiSe and EmissioNs of supErsoniC Aircraft) project (2021–2024) aims to develop detailed models of the produced carbon emissions and the landing and take-off (LTO) noise in the vicinity of airports. The project's activities will complement ICAO's efforts towards establishing technical flight test procedures for en route (sonic boom) and LTO noise certifications. Several platforms have been developed within this project: SENECA E-5 business jet (12 pax, cruise Mach number 1.4), SENECA E-19 (10 pax, cruise Mach number 1.6), SENECA Airliner 1.8 (100 pax, cruise Mach number 1.8), and SENECA Airliner 2.2 (100 pax, cruise Mach number 2.2) (Figure 16).

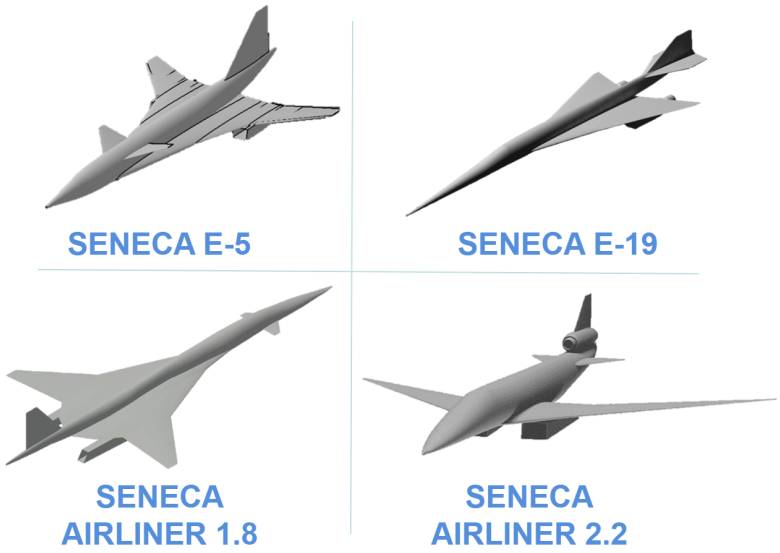

Figure 16. SENECA project concepts.

MOREandLESS (MDO and REgulations for Low-boom and Environmentally Sustainable Supersonic aviation) (2021–2024) is funded by the European Commission under the framework of Horizon 2020, and its main objective is to contribute to define new standards for supersonic aviation that is expected to be environmentally sustainable, for what con-

cerns noise, pollutant and greenhouse gas emissions. A multidisciplinary analysis will include aerodynamics, propulsion systems, emissions and climate impact sciences, with the aim of developing guidelines. New types of fuel, such as biofuel and liquid hydrogen, will be tested [145]. The GreenHawk3 aircraft concept, a 20 pax business jet cruising at Mach 3 resulted from the consortium work, is shown in Figure 17.

Figure 17. GreenHawk3 aircraft concept developed within MOREandLESS project. (Source: [146].)

At present, however, there are still several open questions regarding which is the sonic boom level that could be 'accepted' by the community, which are the effects of repeated sonic booms on humans, animals and buildings, and which metrics should be used to define standard requirements. In any case, companies and airlines have made large investments in the design and development of future, low-boom supersonic aircraft. A number of supersonic concepts, mainly business jets, have been proposed in the last 20 years mostly by start-ups, and some of them already entered, or are going to enter soon, their manufacture and test phase. Aerion Corporation introduced in 2004 an efficient and environmentally friendly supersonic business jet, AS1 (or Aerion SBJ) [147] (Figure 18a). It was a twin-engine aircraft, able to transport 8–12 passengers up to Mach 1.6 and up to 4.000 nm. Its key enabling technology, the supersonic natural Laminar flow wing, was conclusively demonstrated in transonic wind tunnel tests and in supersonic flight tests conducted in conjunction with NASA. In 2014, a larger redesign able to reduce engine emissions was announced. AS2 (Figure 18b) was a triple-engine 12-passenger aircraft aimed for Mach 1.4 for a minimum projected range of 4750 nm. The range and cabin width were increased at the cost of a significant rise in take-off weight. In 2017, a third redesign was published (Figure 18c).At the beginning of 2021, Aerion announced a 50-seat high supersonic-hypersonic airliner project. AS3 (Figure 18d) aimed to achieve speeds of Mach 4 or more and a range of 3800 nm. However, in May 2021, the company shut down due to inability to raise capital.

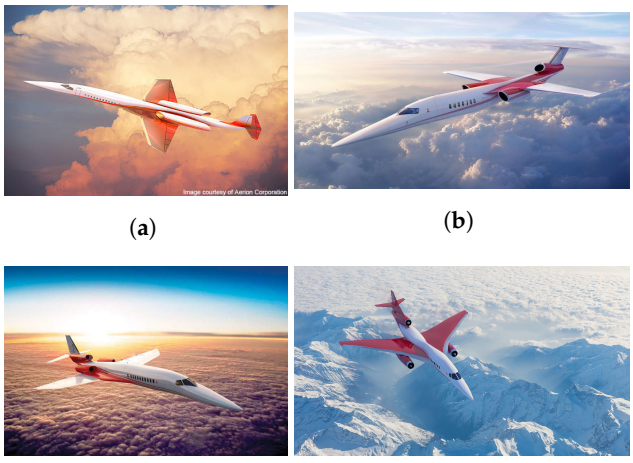

(**a**) (**b**)

(**c**) (**d**)

Figure 18. Aerion AS-1 (**a**) (Source: [148]), Aerion AS-2 (**b**) (Source: [149]), Aerion AS-2 redesigned (**c**) (Source: [150]) and Aerion AS-3 (**d**) (Source: [151]).

Spike Aerospace proposed in 2014 the S-512 (Figure 19a). It was a twin engine, designed for 12–18 passengers, Mach 1.8 for a range of 4000 nm. The proposal was considered unattractive and was replaced in 2015 by another version (Figure 19b). The range was increased by more than 50% and take-off weight went up from 36.2 to 52.2 tonnes [152] and Mach reduced to 1.6. The wing was completely redesigned, and the position of the two engine changed from upper to side fuselage. The aircraft does not expect cabin windows; instead, it will be lined with tiny cameras sending footage to thin, curved displays lining the interior walls of the fuselage for noise reduction [153]. Spike claimed the aircraft would be able to create a sonic boom with a perceived loudness of less than 75 dB at the ground level [154].

(**a**) (**b**)

Figure 19. Spike S-512 (**a**) (Source: [155]) and its redesign (**b**) (Source: [156]).

Another promising concept aircraft is the Boom Overture (Figure 20a) from Boom Supersonic, founded in Denver in 2014. The Overture is supposed to travel at Mach 1.7, carrying 65 to 88 passengers for 4000–4500 nautical miles, and it is expected to rollout in 2025 and be introduced in 2029 [157]. It would keep the delta wing configuration of Concorde but would be built with composite materials. It would be powered by three dry turbofans [158]. In September 2020, the company announced that it had been contracted to develop the Overture for possible use by Air Force One [159], and United Airlines already placed orders for 15 aircraft [160]. The company is also working on the XB-1 Baby Boom (Figure 20b), a one-third-scale supersonic demonstrator, designed to fly at a cruising Mach of 2.2, with over 1000 nm of range, and powered by three engines [158]. Its main objective is to pave the way for mainstream supersonic travel by demonstrating the key technologies for safe and efficient high-speed flight. It is expected to be flight tested in 2021 [157].

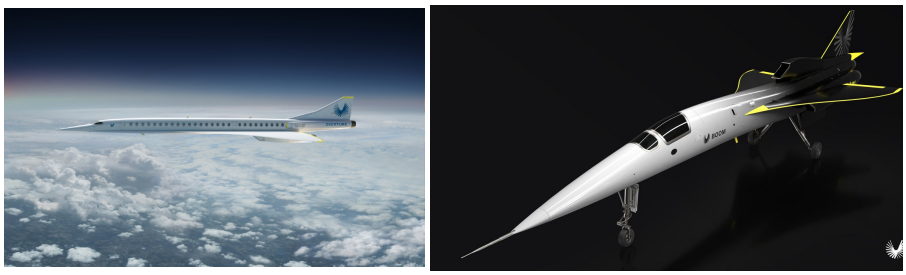

(**a**) (**b**)

Figure 20. Boom Overture (**a**) (Source: [161]) and Boom XB-1 (**b**) (Source: [157]).

NASA X-59 QueSST (Figure 21) is the result of the Low-boom Flight Demonstrator (LBFD) project. This experimental aircraft, manufactured by Lockheed Martin Skunk Works, is a single-engine aircraft, designed to cruise at 1.4 Mach at 55,000 ft [162]. NASA claimed the X-59 will produce very low sonic boom (60 dB), about 1/1000 as loud as current supersonic aircraft, enabling the possibility of flying supersonic overland. This

is achieved by using a long, narrow airframe and canards to keep the shock waves from coalescing [163], and a top-mounted intake, even if the inlet flow distortion, due to vortices, represents a concern [164]. The X-plane was expected to start flying in 2022 over select U.S. communities to gather data on human responses to the low-boom flights and deliver that data set to U.S. and international regulators [165].

Figure 21. NASA X-59 QueSST (Source: [166]).

Another Quiet Supersonic Transport aircraft effort was pursued by Supersonic Aerospace International (SAI) with the QSST-X: the design focused on supersonic technologies that will ensure a low boom signature. The project was announced around the year 2000, and Lockheed Martin Skunk Works was contracted to begin the development in 2001 [167]. Designed to cruise at an altitude of 60,000 feet at speeds of Mach 1.6 to 1.8, with a range of 4600 nm, the two-engine aircraft features a gull-wing, a canard and an inverted V-tail (Figure 22a) to create a sonic boom only 1% as strong as that generated by the Concorde [168], by limiting the signature coming off of the back of the aircraft. In 2013, Supersonic Aerospace International relaunched the concept as much larger Boeing 737-sized aircraft to operate as an all-first-class airliner [169]. The company redesigned the aircraft (Figure 22b) by providing extra passenger cabin size and capacity, including a convertible airliner/business jet seating configuration, extra range capability (over 5000 nm at Mach 1.6) and by implementing advanced bio-fuel-efficient engines. It is claimed to have exceptionally quiet and environmentally sound performance, and to represent a quantum leap advancement in aviation technology for the '21st Century' [170].

(**a**) (**b**)

Figure 22. SAI QSST first (**a**) (Source: [171]) and second (**b**) concept (Source: [169]).

In the end, HyperStar (Figure 23) by HyperMach is a proposed supersonic jet airliner, announced in 2011 as SonicStar, expected to reach speeds of up to Mach number 3.6 [172] with a range up to 6000 nm. It is planned to be powered by two engineered SonicBlue HYSCRAM (Hypersonic Superconducting Combustion Ram Accelerated Magnetohydrodynamic Drive) hybrid hypersonic 6500-X series engines [173]. Sonic booms are expected to be eliminated overland by using an electromagnetically induced plasma wave that "absorbs" pressure waves through a magnetic spike on the nose [174]. The proposed SonicStar would carry 10 to 20 passengers [175]. Recently, in 2012, the company changed the aircraft

specifications, increasing the SSBJ top speed estimate to Mach 4.5 and range to 6500 nm, and renamed the aircraft to HyperStar. It also increased the size of the airplane to seat up to 36 passengers [176]. In 2016, HyperMach once again revised the aircraft's preliminary performance and specifications upward, to a top speed of Mach 5 at 80,000 feet and 7000 nm range [177]. The jet will not fly until about 2025 [174], with certification and entry into service slated to follow in 2028.

Figure 23. HyperMach SonicStar (Source: [177]).

Figure 24 provides a summary of the various projects and supersonic aircraft concepts described above.

Company	Aircraft Concept and features	Year	Country	Sonic Boom Performance Expected
DARPA (Defense Advanced Research Projects Agency)	Slender Body Conventional Configuration	2000	USA	N/A
Supersonic Aerospace International & Lockheed Martin Skunk Works	QSST-X gull wing, canard and inverted V tail configuration	2000	USA	1% of Concorde boom level
DARPA & NASA	SSBD Northrop F-5E shaped for low boom	2001-2003	USA	1/3 boom reduction with respect to F-5E
Aerion Corporation	AS-1 AS-2 AS-3 Slender body swept wing configuration with supersonic natural laminar flow wing	2004, 2014, 2017 (Shut down in 2021)	USA	N/A
European Consortium	HISAC Low noise and low boom optimized Configurations	2005-2009	Europe	N/A
NASA & Gulfstream	F15B aircraft equipped with Gulfstream patented Quiet Spike X54 quiet spike swing wing configuration	2008	USA	75 dB boom loudness at ground
JAXA (Japan Aerospace Exploration Agency) & SKY Aerospace	DSEND#2 Silent supersonic Concept Model Cranked arrow wing with supersonic laminar flow and non symmetrical fuselage supersonic business jet	2010-2015	Japan & India	N/A
HyperMach	HyperStar Mach 4.5-5 delta wing slender body configuration equipped with a magnetic spike for sonic boom elimination	2011	USA	
Spike Aerospace	S512 slender body cranked wing (straight wing in its reshaped version) configuration with no cabin windows for noise reduction purposes	2014	USA	<75 dB boom loudness at ground
NASA & Lockheed Martin Skunk Works	X-59 QueSST low boom demonstrator canard wing tail configuration adopting an integrated airframe-engine design	2018	USA	60 dB boom loudness at ground
European Consortium	SENECA Low LTO noise and boom configurations	2021-2024	Europe	N/A
European Consortium	MOREandLESS Low boom and LTO noise Hypersonic Aircraft Concepts (GreenHawk3 and STRATOFLY MR3)	2021-2024	Europe	N/A

Figure 24. Supersonic aircraft projects and concepts table summary.

It is well known that one of the keys to eliminating sonic booms is the design of the airframe. Sonic booms at the ground are mainly caused by the coalescence of shock waves as they propagate from the aircraft thorough the atmosphere. In a conventional supersonic jet, the shock waves coalesce as they expand away from the nose and tail, leading to two distinct sonic booms (N-waveform). For this reason, the exploration of unconventional configurations, enabled by the capability of using advanced computational methods at the early stages of the design process, could be a key element in shaping the future "boomless" supersonic aircraft. In the next subsections, configurations worth being explored further in the future are described.

3.2.2. Forward-Swept Wing Configuration

A forward-swept wing is an aircraft configuration in which the wing, instead of being swept in a positive way (backward), is swept forward, or has a negative sweep angle. Such a configuration provides advantages, especially in terms of maneuverability and controllability at high angles of attack but comes with the aeroelastic issue of reduced divergence speed. Today, the use of composite materials to avoid the problem of reduced divergence speed through aeroelastic tailoring and the advent of fly-by-wire technology that allows for the design to be dynamically unstable makes the forward-swept wing configuration a practical design. Examples of aircraft with a forward-swept wing are Grumman X-29 technology demonstrator, the Sukoi Su-47 fighter prototype and the KB SAT SR-10 trainer aircraft prototype (Figure 25).

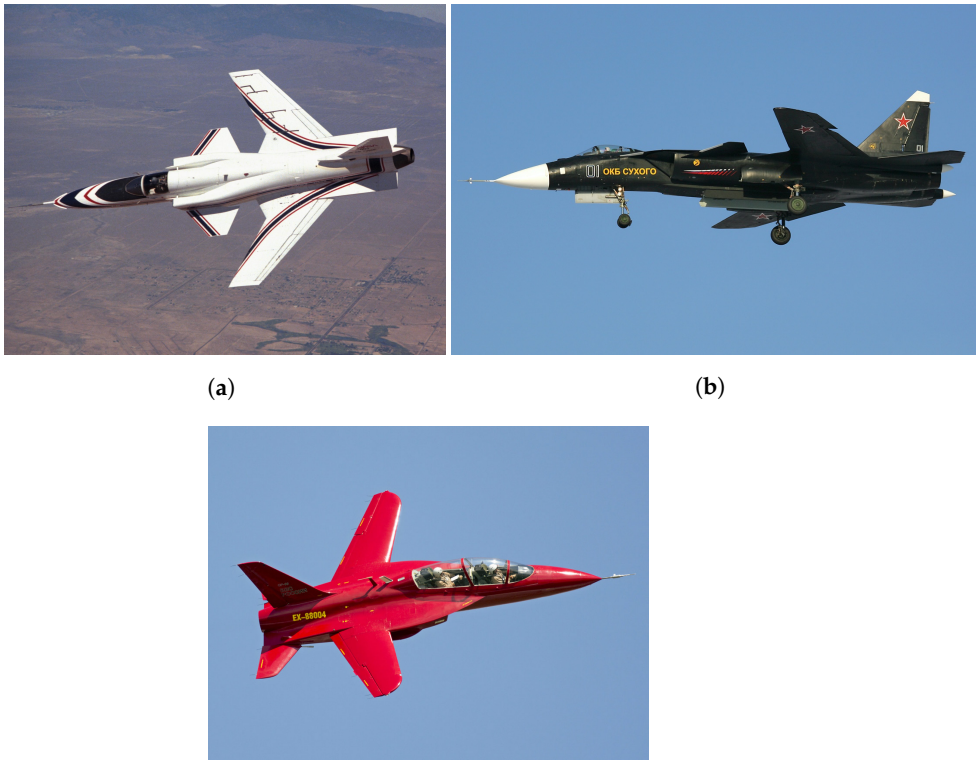

(**a**) (**b**)

(**c**)

Figure 25. Grumman X-29 (**a**) (Source: [178]), Sukoi Su-47 (**b**) (Source: [179]) and KB SAT SR-10 (**c**) (Source: [180]).

Regarding the design of the low-boom supersonic aircraft, the forward-swept wing configuration seems to be promising as highlighted in several works. In [181], Kishi, Makino and Kanazaki investigated both the aerodynamic and sonic boom performance of 13 wing-body-engine nacelle configurations with varying wing platforms for a supersonic business jet. The calculated results for supersonic cruise conditions indicated that the maximum acoustic level of the sonic boom of a forward-swept wing was approximately 4.8 PLdB

lower than that of the backward-swept wing. Furthermore, a forward-swept wing reduced the aerodynamic drag as effectively as a backward-swept wing during supersonic cruising. The sonic boom signature at the ground level indicated that forward sweeping of the wing caused multi-peaks on the bottom peak of the trailing sonic boom, demonstrating that it could reduce the intensity of trailing sonic boom. In [120], a multi-objective optimization study was carried out by selecting low wave drag and low boom values as objective functions. Optimization results indicate that a swept forward wing configuration has benefits in both boom and wave drag reduction because the lift distributions of such a wing configuration are well distributed along the fuselage axes, and the cross-area distributions are smoother than the sweptback wing. This behavior is well shown and explained in a patent [182] for a variable forward-swept wing supersonic aircraft. As shown in Figure 26, by adopting a forward-swept wing, lift is generated from a more forward position than in the case of a backward-swept wing. This causes an increase in the equivalent cross-sectional area in the forward half of the aircraft body, due to the increase in the equivalent cross-sectional area due to the lift, which compensates and adjusts the equivalent distribution of a conventional aircraft to meet the Darden [110] ideal equivalent cross-sectional area distribution for minimizing low-boom characteristics. Moreover, cross-sectional area distribution changes are very small, maintaining it near the Sears–Haack body and, therefore, does not increase the wave drag.

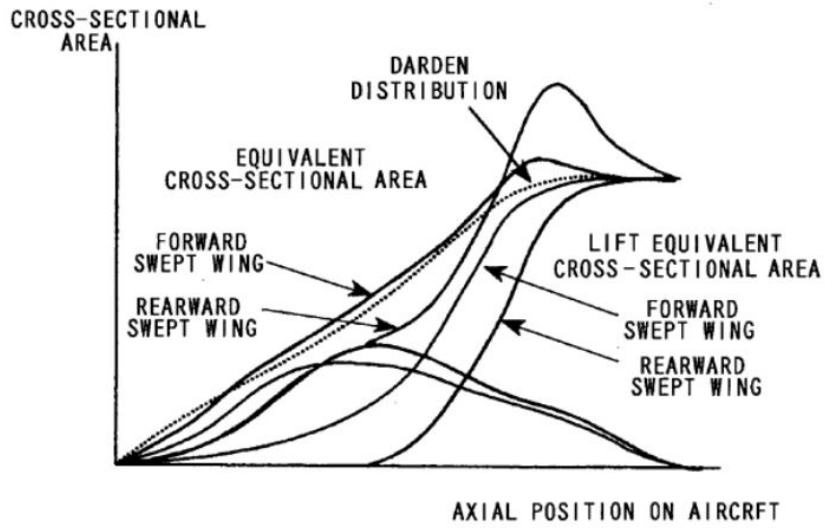

Figure 26. Equivalent cross-sectional area distributions of a rearward-swept wing, forward-swept wing and ideal Darden distribution (Source: [182]).

The patent presents an aircraft with a variable forward-swept wing in which the forward sweep angle could be changed during different flight phases, with the aim of tailoring both aerodynamic and sonic boom performance. The variable forward-swept wing could also provide an advantage in regard to the increase in the trim drag that is accompanied by the rearward movement of the aerodynamic center during supersonic flight: the effect of this movement, in fact, can be canceled by increasing the wing forward sweep angle so that the aerodynamic center is moved forward; as a result, the trim drag can be minimized [182]. Another advantage of a forward-swept wing configuration is that it allows the wing spar carry-through to go behind the cabin, further increasing its size. This could be important either to accommodate more passengers (airliner) or to increase the comfort (business jet). Drawbacks associated with sweeping the wing forward are connected with the requirement of a far greater amount of structural stiffness and the increased structural weight by the aeroelastic tailoring effect. However, by exploiting fiber composite materials of high stiffness and adjusting them differently in different directions, the weight penalty could be 'minimal' [183].

3.2.3. Oblique Wing Configuration

The oblique wing configuration seems to be another promising concept for future supersonic aircraft both in terms of aerodynamic performance and sonic boom at low Mach numbers. R.T Jones, in 1956 [15], was the first to study this concept: he suggested that aircraft with asymmetrically swept (oblique) wings would offer many advantages at high transonic and low supersonic speeds. The main advantage related to the oblique wing arrangement is that it effectively has twice the wing length as a symmetrically swept wing of the same span, sweep and volume, which offers a reduction in both volume and wave drag, as shown in Figure 27. Moreover, it might achieve twice the fuel economy of more conventional wings since higher supersonic L/D can be achieved.

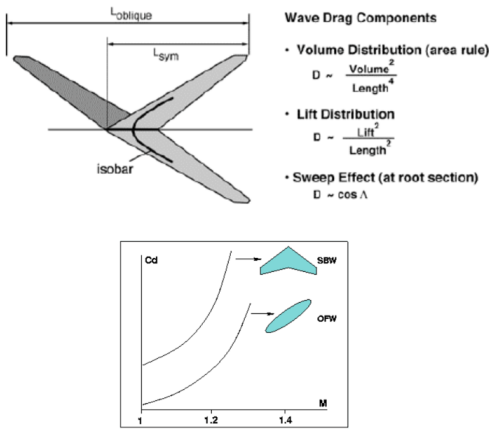

Figure 27. Oblique wing geometry and wave drag compared with a swept wing (Sources: [184,185]).

Jones's various papers have shown that the oblique wing can be realized in several different ways. In its purest form, it can be simply a flying wing (OFW) at an oblique angle. Alternatively, the wing can also be placed on a normal fuselage (OWB) and fixed permanently at a particular angle, or center-pivoted to a fuselage, allowing the angle to be changed as desired. First investigations on aerodynamics and performance of the oblique wing have been made by NASA. A demonstrator, the AD-1 (Figure 28), was built and flown in 1979 to test the oblique wing-body concept in various oblique configurations, evaluating a pivot wing concept and gathering information on handling qualities and aerodynamics at various speeds and sweep angles [186].

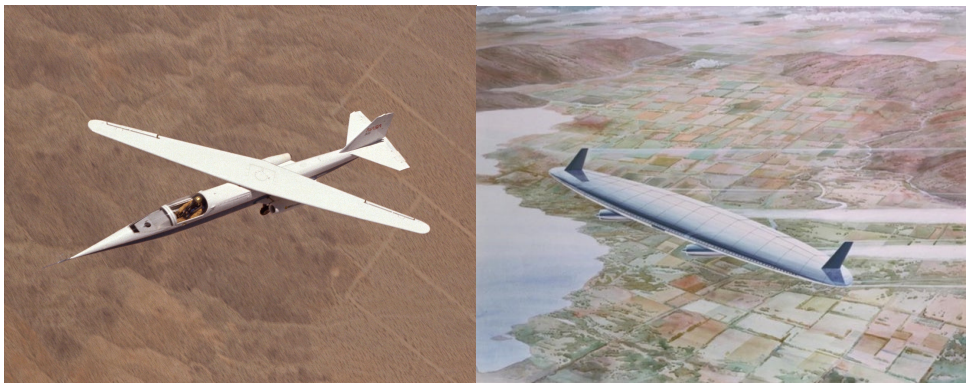

Figure 28. The AD-1 aircraft in flight with its wing swept at 60 degrees, the maximum sweep angle (**left**) (Source: [186]) and an artist concept of oblique flying wing by NASA (**right**) (Source [187]).

Since the equivalent area distribution of the wing is better spread out longitudinally, a near-cylindrical passenger cabin can be used. The straight carry-through structure of the oblique wing avoids torques that are usually reacted by the fuselage structure and

so makes the structure simpler. The oblique wing could also mitigate the sonic boom by generating favorable combinations of more uniform lift and volume distributions along the vehicle length. Wind tunnel tests [188] were conducted to determine the magnitude of the ground track sonic boom overpressure generated by an oblique wing transport aircraft cruising at Mach 1.4 at 45,000 ft. Results confirmed that the oblique wing configuration has lower sonic boom overpressure levels at cruise lift coefficient than a swept wing. Works on oblique flying wings highlighted that bow shock overpressure is typically one-third less than comparable symmetric configurations. The aft-shock is canceled due to favorable volume–lift interference [189]. However, due to the unsymmetrical shape of the aircraft, the waves vary strongly with the azimuth angle, which will result in significant asymmetry in the magnitude and duration of the sonic boom in both near and far fields [190]. Many of the technical challenges of oblique wings arise from their nonlinear and strongly coupled aerodynamic characteristics. Significant variations in the rolling moment with changes in the angle of attack are observed; unusual inertial couplings and aeroelastic characteristics further complicate the dynamics; and for certain oblique wing configurations, propulsion integration is problematic [184]. The asymmetry of the geometry also causes some stability and control issues, which offers challenges in the control system design.

3.2.4. Supersonic Biplane

Another interesting option for a low-drag low-boom supersonic aircraft is the supersonic biplane. Proposed for the fist time by Busemann in 1935 [191] as a configuration that can eliminate over 80% of show waves, it has drawn the interest of several researchers that have conducted 2D and 3D simulations to assess and optimize this configuration. Busemann's supersonic biplane concept is shown in Figure 29: it does not generate wave drag in inviscid supersonic flow thanks to the interference of shock and expansion waves (wave cancellation effect). Since the pressure does not change, even the sonic boom associated with the wing is canceled, leading to a boomless configuration. The Busemann biplane, however, does not work in lifting conditions, and its performance at off-design Mach numbers can be very poor due to the choked flow and flow hysteresis problems [192].

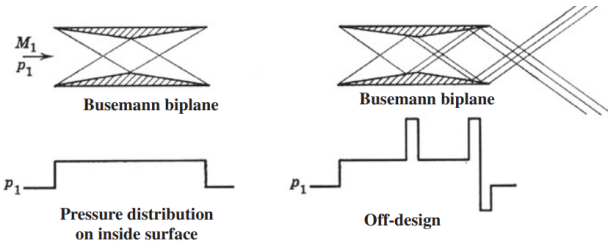

Figure 29. Busemann supersonic biplane concept in both design and off-design conditions (Source: [193]).

At lifting conditions, the aforementioned concept can be expanded to Licher's supersonic biplane concept [194]. A typical Licher biplane, shown in Figure 30, is asymmetrical and can be divided into the Busemann part and the additional part. The wave drag due to lift can be reduced to 2/3 of that of a single flat plate under the identical lift condition, and the Busemann wave cancellation concept can be applied as well to eliminate wave drag due to airfoil thickness [192]. The Licher biplane, whose thickness/chord ratio of the lower element is bigger than the ratio of the upper element, provides a larger lift/drag ratio (L/D) than the Busemann biplane at lifting conditions [195].

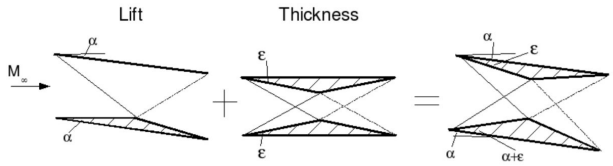

Figure 30. Licher biplane concept (Source: [196]).

Optimized biplane airfoils [193] or the usage of hinged leading edge and trailing edge flaps to increase the ratio of the throat area to the inlet area [197,198] could reduce dramatically the effects of the choked flow and flow hysteresis phenomena, while maintaining a certain degree of favorable shock wave interaction effects at the design Mach number.

A new design for the supersonic biplane shown in Figure 31 was developed in 2020 [199], which improves aerodynamic performance in both design and off-design conditions. It consists of an isosceles triangle airfoil and a flat plate, and has the aerodynamic advantages of lower drag, higher lift-to-drag ratio, and a weaker flow-choking phenomenon than the Busemann biplane. Further analyses, especially in sonic booms, are required to assess its suitability for designing future supersonic aircraft.

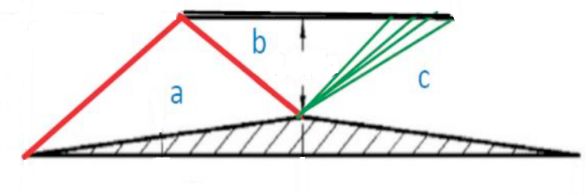

Figure 31. Sketch of new biplane concept: in red shock waves are sketched, while in green expansion waves are sketched.

CFD simulations [200,201] and wind tunnel tests [202] have demonstrated that the three-dimensional Busemann biplane has a weaker flow-choking problem than the two-dimensional Busemann biplane due to the three-dimensional effect, but at the same time, it requires winglets to maintain the wave interactions at wingtips and prevent large drag penalties [203]. Biplane wing performance can be increased by optimizing the planform characteristics, such as taper ratio and aspect ratio [200,201]. Regarding sonic boom performance, Utsumi and Obayashi in [204] highlighted that, according to linearized flow theory, the equivalent area distribution of the biplane due to the volume could be reduced significantly or even canceled in fully three-dimensional nonlinear supersonic flows. It is, on one hand, beneficial for sonic boom performance because the wing contributes just with the lift; on the other hand, it allows increments in the cross-sectional area of the fuselage without increasing the total equivalent area distribution, making room for passengers larger. A concept for a Busemann supersonic biplane aircraft by Tohoku University is shown in Figure 32a, while Figure 32b represents the design of a biplane twin body aircraft by JAXA and Nagaoka University. The latter design, in particular, has been analyzed in several papers [195,205,206], resulting in a very promising candidate for the next generation of supersonic airliners. In fact, according to their results, the biplane wing concept and the twin-body fuselage concept have significant individual drag reduction effects. Approximately 150 cts drag reduction is achieved by the adoption of the biplane wing configuration, and then, separately, about another 60–80 cts drag reduction is achieved by the adoption of the twin body fuselage configuration. Moreover, sonic boom performance is also good in terms of both overpressure and loudness, with the best configuration having a maximum pressure rise 38% lower than the conventional single-body/diamond-wedge wing configuration. The sonic boom performance parameters become better with the adoption of the biplane wing configurations, while the fuselage body configurations seem to have less effect.

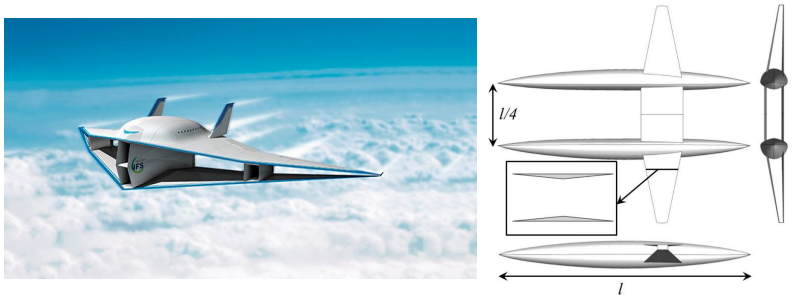

(**a**) (**b**)

Figure 32. Concept of supersonic biplane (**a**) (Source: [207]) and supersonic biplane twin-body aircraft (**b**) (Source: [208]).

3.2.5. Supersonic Bi-Directional Flying Wing

A revolutionary concept, intended to break through the technical barriers of conventional supersonic tube-wing configurations, is the Supersonic Bi-Directional Flying Wing (SBiDir-FW). Designed by Professor Zha [209] from the University of Miami, the project was picked up by NASA as part of its Innovative Advanced Concepts Selected For Continued Study program. According to the first design stages, analyses and trade studies made by Zha and his research group [210–212], the bi-directional flying wing has the potential to revolutionize supersonic flight with virtually zero sonic boom and ultra-high aerodynamic efficiency in both subsonic and supersonic flight phases. The novel planform, shown in Figure 33, is symmetric about both the longitudinal and span axes. For supersonic flight, the planform can have as low of an aspect ratio and as high of a sweep angle as desired to minimize wave drag and sonic boom. For subsonic mode, the aircraft is expected to rotate 90 deg to achieve superior stable aerodynamic performance, with a low sweep angle and high aspect ratio. In such a way, the conflict of the subsonic and supersonic aerodynamic performance of the conventional fuselage-wing configuration is hence removed. The desirable transition mode Mach number is high subsonic (about 0.8) to avoid the unsteady force introduced by shock waves at supersonic speed. The engines are not rotated and maintained always in alignment with the flight direction. The yaw moment to rotate the airframe is generated by ailerons or flaps on the two sides of the flying wing. Therefore, a dedicated power driven system to rotate is not required, avoiding the weight penalty and system complications to the design. The time required for the transition between modes can be controlled to be about 5 to 10 s: it appears to be short enough so that from an inertia point of view, neither the momentum nor lift should be affected.

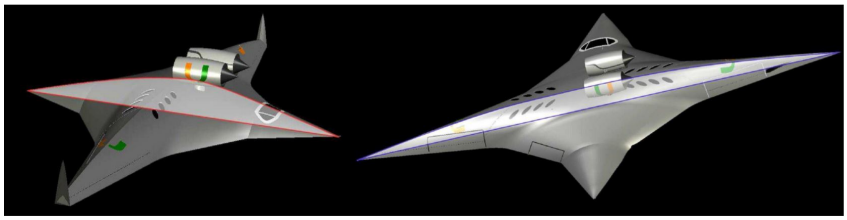

Figure 33. SBiDir-FW Planform flying in subsonic (**left**) and supersonic (**right**) mode (Source: [211]).

Concerning aerodynamic performance and sonic boom, the preliminary CFD simulation [210] for a SBiDir-FW business jet (BJ) at Mach numbers of 1.6 and 2.0 indicates that the configuration generates no N-wave sonic boom on the ground at a high lift-to-pressure drag ratio L/D of 16. The platform adopts a sharp nose and an isentropic compression pressure surface, which minimize the shock wave propagating downward and the resulting sonic boom. The maximum overpressure at the ground is found to be 0.3 psf at the design angle of attack (0 deg) and 0.9 psf for an angle of 1 deg, which is the required cruising angle of attack to provide the optimal L/D. Further analyses and trade studies are presented in [212]. It is discovered that the airfoil meanline angle distributions are critical to mitigate

far-field sonic boom, whereas the sweep angle determining the aspect ratio has a strong effect on aerodynamic efficiency. In particular, by using nonlinear and non-monotonic meanline angle distribution, the sonic boom ground loudness can be reduced by over 20 dBPL, achieving less than 70 dBPL. The numerical results obtained so far demonstrate that the SbiDir-FW could be a very promising concept for supersonic flight.

3.3. Noise Reduction Systems and Technologies

Ways of reducing or even eliminating sonic booms has been an area of interest both in industrial and academic domains since the 1960s. The first and most intuitive concept of mitigating the boom is by shaping the aircraft. Shaped sonic boom signatures can achieve a reduction in loudness of 15–20 dB or higher with no added energy beyond that to sustain flight. Details of sonic boom minimization theory and techniques are given in Section 2.3. However, shaping the aircraft for low-boom purposes could lead to increased manufacturing costs. In addition, the curved shaped body strongly perturbs the airstream flowing around the aircraft, affecting not only the aerodynamic characteristics but also the weight and useful volume. An acceptable compromise is difficult to find, especially in the case of large aircraft [213]. Recently, some innovative and exotic concepts have been proposed to reduce the sonic boom and wave drag of supersonic aircraft.

3.3.1. Nose Spike

One of the most promising sonic boom reduction systems is the Gulfstream Aerospace patented [214] Quiet Spike concept. The Quiet Spike is an extendable nose spike developed to alter the shock wave field ahead of the aircraft. It works by breaking up the single large nose shock into a stair-stepped series of discrete small shocks [215] (Figure 34b). The series of weak shocks generated by each of the telescoping sections will not coalesce into an N-wave but propagate to the ground in parallel fashion. The system is supposed to be retracted in low-speed flight phases and fully extended at supersonic speed. A supersonic jet equipped with the nose spike is shown in Figure 34a in a fully extended configuration. Numerical simulations and several wind tunnel tests [216,217] have been performed to assess Quiet Spike performance and feasibility. Gulfstream and NASA cooperated in the flight trails which aimed to test the effect of the Quiet Spike in sonic boom mitigation. The Quiet Spike was adapted to an F-15B flight research aircraft, and a total of 32 research flights were conducted [218–220]. The Quiet Spike has been shown to be capable of achieving a 0.2 psf initial shock reduction and an increase of 25% in rise time [216]. It has proven its capability of playing a significant role in achieving the desired area distribution for a low-boom aeroplane. The main drawbacks associated with this system are related to the complexity of the telescopic design: it requires, in fact, a very sophisticated and reliable mechanism able to be extended and retracted in flight. In addition, it consists in a weight and power penalty, higher manufacturing costs and failure risks. Hence, the challenges associated with designing the Quiet Spike include minimizing weight and maximizing stiffness as well as providing adequate aeroelastic stability [215].

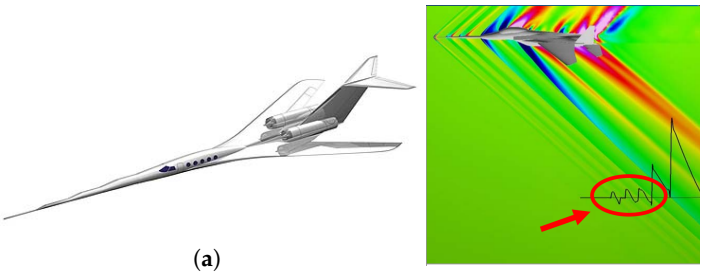

(**a**) (**b**)

Figure 34. Quiet Supersonic Jet High Speed Configuration with Quiet Spike (**a**) (Source: [154]) and CFD analysis of Quiet Spike structure (**b**) (Source: [221]).

3.3.2. Shock Wave Dispersion

Shock wave dispersion is another concept developed to help in achieving acceptable sonic boom. This technology aims to disperse shock waves over a larger area to have lower pressure levels at the ground than in the clean case. The dispersion is achieved by means of low amplitude vibration of aircraft nose, wing and tail leading edges obtained mechanically or electrically. In this way, the stationary characteristic of the shock wave effect is canceled and substituted with a transient state, reducing the effect of sonic booms on the ground surface. In [222], the author proposed this method for the first time: the dispersion of the shock waves is produced through periodical small variations of the semi-angle α of the aircraft surfaces that lead to a much larger variation of the shock wave angle β. The working principle is shown in Figure 35.

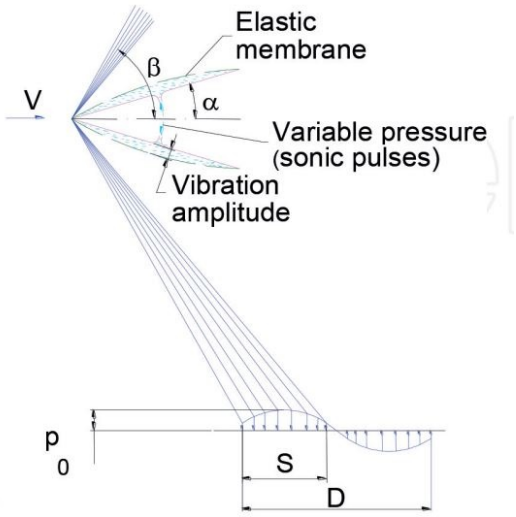

Figure 35. Dispersion of shock waves by membrane vibration (Source: [213]).

The system could be realized in different ways. One possibility is to vibrate the surface by means of a membrane actuated by pulses propagated in a hydraulic liquid. When pressure pulses of a certain frequency are injected in a liquid through perforations in wing LE, the membrane begins to vibrate with the same frequency. The pressure pulses can be produced by sonic equipment. The results obtained in [213] show that through dispersion, especially for Mach numbers between 1 and 1.8, the footprint is enlarged about 23 times. Furthermore, even larger dispersion distances can be obtained if the semi-angle α is taken equally to the limit angle α_{lim} for detaching the oblique shock wave. It is highlighted that the effective period of membrane oscillation should be smaller then the average duration of a natural N-wave. Another possible means of dispersing shock waves could be to substitute the membrane by an elastic fairing made of thin carbon fiber composite or by high-voltage electrodes, the so-called plasma actuators that affect the airflow through air ionization. Plasma actuators are also researched for noise reduction in fan ducts. The latter solution, however, seems to be unfeasible for large-scale applications, as in the case of a real aircraft. Another new possibility proposed in [213] is dispersing through the injection of electrons in the surrounding airflow by means of sharp electrodes (Figure 36).

The cathodes are sharp Wolfram needles placed along a rod, which is fixed in the tip of aircraft nose and along the wing LE. The anodes are thin copper sheets, which are fixed by the aircraft nose and pressure/suction sides of wing. A high-potential electrical source (thousands of volts) is connected to the cathodes and anodes: when it is connected, a high number of electrons are released through the sharp tips of the cathodes. Because inside the shock wave, due to the very small space, the density of electrons and temporary negative molecules is high as a result of electrostatic repelling forces, the shock wave thickness increases, and its impact at ground level is mitigated. After passing through the shock wave, the airstream is neutralized by the anodes placed on the aircraft nose and wing,

which collect the electrons present in the air stream. According to the author [213], shock wave dispersion represents a concrete alternative for shaping technology that has, as a main disadvantage, the high deviation of air stream around the aircraft, requiring an increase in propulsion power as a result. Furthermore, it should also be investigated much more to assess its feasibility for real applications.

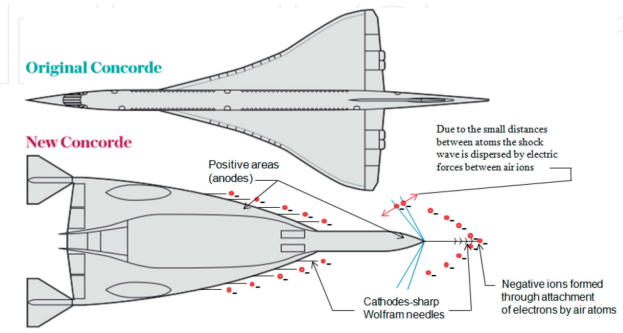

Figure 36. Solution proposed for dispersing of shock wave through the injection of electrons in surrounding airflow by sharp electrodes (Source: [213]).

3.3.3. Jet Stream

A patent released in 1973 [223] presents a means of weakening the wing shock wave by creating a strong interaction between the shock wave and a high speed jet stream, called the anti-boom jet, generated toward it. The jet stream produced is of approximately equal pressure but a higher Mach number than the ambient supersonic flow and is directed toward the wing shock wave below the wing leading edge (Figure 37a). The high-speed jet stream intercepts the wing shock wave and produces an intense interaction (Figure 37b). The interaction creates a pressure profile on the underside of the wing which maintains and, under proper conditions, may improve the lift. The shock wave that emerges from the high speed jet stream is a refracted continuation of the leading wing shock, and is weaker than the wing shock without interaction. This weakened wing shock will propagate into the ambient atmosphere at a lesser velocity so that the boom signature at the ground level will be altered since the wing shock wave, which normally reinforces the leading nose shock wave, will now be shifted aft-ward and separated from the leading nose shock. The slightly weakened and shifted wing shock will rise from a lower pressure level in the boom signature and reach a maximum overpressure at a level lower than that resulting when the wing shock and nose shock are superposed. The maximum underpressure in the rear half of the boom signature can likewise be reduced, and the boom signature will be stretched out downstream. Since a major portion of the fluid flux in the anti-boom jet can be air economically captured from the ambient atmosphere, the main thrust-producing engines of the aircraft with power capacity available may contain all the elements required to produce the jet and can be conveniently used for the purpose if properly located. Also, the engines exhaust may be used with the anti-boom jet in weakening the wing shock wave.

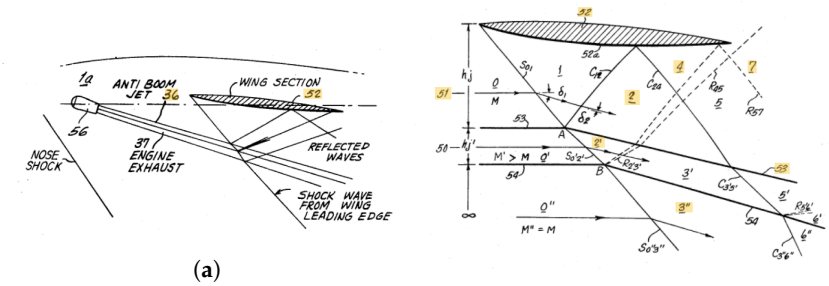

(**a**) (**b**)

Figure 37. Interaction of a wing leading edge shock wave with a contact discontinuity produced by a stream of higher Mach number than the airstream (Source: [223]).

3.3.4. Flow Suction and Injection

Another system for sonic boom reduction was presented in 2021 by Ye et al. [224]. It consists of equipping the wing leading edge with a suction slot and the trailing edge with an injection slot as shown in Figure 38. Analyses have been carried out on both diamond and NACA0008 airfoils to assess the capability of the device. Moreover, the effects of the suction and injection location, the suction and injection slot size, the mass flow rate and the attack angle on the ground boom signature and drag coefficient have been studied in detail. The results showed that the suction–injection device has benefits in both sonic boom and wave drag reduction, avoiding weight penalty and sacrifice of fuselage space. Furthermore, the method has the advantages of simple operation and easy control, and is effective also for off-design angles of attack. For energy saving, the suction and injection slots are opened when the supersonic aircraft flies over the city, and they are closed when the aircraft flies over the sea.

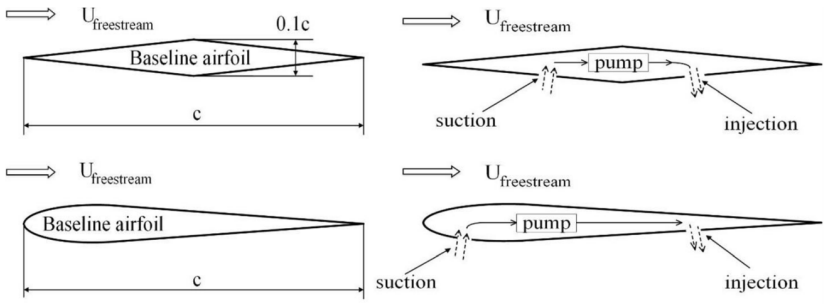

Figure 38. Baseline diamond and NACA0008 airfoils (**top**) and optimized diamond and NACA0008 airfoils with both suction and injection (**bottom**) (Source: [224]).

3.3.5. Energy and Heating Addition/Cooling

Miles et al. [225,226] proposed active sonic boom suppression through off-body dynamic and pulse energy addition. This approach could reduce the far-field signature primarily by suppressing the far-field coalescence of the various shock waves originating from the different parts of the vehicle. In these studies, the optimal location of a pulsed shock based on less power consumption and the suppression of far-field shock waves were investigated, as well as the effect of energy release to attenuate the sonic boom on the ground. By apparently increasing the length of the airplane, an initial rise of 0.8 psf is reduced to 0.2 psf with a peak rise of 0.6 psf. In [227], Potapkin and Moskvichev introduced a numerical study about the possibility of reducing the sonic boom level by locally releasing heat to a supersonic gas flow at a Mach number equal to 2 ahead of the body. Different magnitudes of heat supply to the incoming flow were tested. The computational results show that the local heat supply to the flow ahead of the body can reduce the sonic boom level by more than 20%. The reduction in the sonic boom level is ensured by changing the free-stream parameters ahead of the body and by preventing the coalescence of shock waves from the heat supply zone and from the body in the far field. Methods of energy supply to a supersonic flow by means of laser and microwave radiation, electron guns, and electric arc discharge successfully applied for modeling flow control processes were also investigated [228,229].

In [230], instead, the method of energy removal (cooling) for the purposes of drag and boom reduction was examined. Surface cooling is shown to exert a significant effect on the formation of the disturbed flow structure up to large distances from the body by an example of a supersonic flow around a body of revolution. The capability of controlling the wave structures formation process, such as hanging shocks formed in the immediate vicinity of the surface, inducing them by means of surface cooling in the region of shock waves nucleation, is demonstrated. Cryogenic forcing remains fairly efficient in the disturbed flow up to large distances from the body, leading to a decrease in the sonic boom level of up to 12 %. Comparisons of experimental data and numerical estimates show that the main

mechanism of the cryogenic action on the flow structure is the reduction in the disturbances' propagation velocity near the surface generating them.

3.3.6. Control Lift Devices

Sonic boom mitigation through the implementation of a strake leading edge flap is described in the patent in [231]. The invention shown in Figure 39 is configured to function as a subsonic leading edge, even at supersonic conditions. The strake can be controlled, deflected up and down to control the sonic boom signature, to manage or reduce air spillage, and also to improve drag. The strake leading edge flap can also be controlled to reduce the lift ahead of spillage at an off-design condition while maintaining a low sonic boom signature. According to the inventor, strake leading edge flap and conventional leading edge devices, individually or in various combinations, can operate to shift the lift distribution of the aircraft and to shape the active area distribution in such a way that sonic boom amplitude reduction is obtained at the ground.

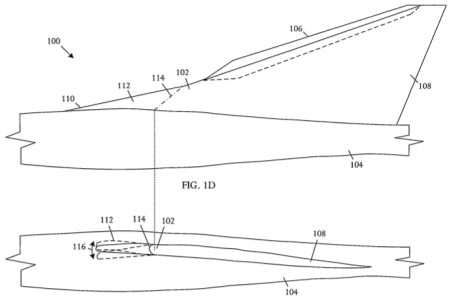

Figure 39. Bottom and side views of an embodiment of a leading edge strake flap (Source: [231]).

Another patent [232] introduced, instead, different ways of generating low boom lift distributions by using both leading edge and trailing edge flaps. Examples are shown in Figure 40. For low-speed flight (e.g., during take-off and landing), the high-boom mode is selected. That is, the flight control system configures the lift control devices to optimize aircraft performance (e.g., optimize L/D and CLmax). For supersonic flight overland, instead, the low-boom mode is selected. That is, the flight control system configures the lift control devices to distribute the lift smoothly over the length of the aircraft and simulate a highly swept wing planform.

In the figure below (Figure 41), a summary of the systems described in this section is provided with an emphasis on the advantages and drawbacks of each one. TRL is also evaluated.

3.4. Critical Review

Three ways of reducing sonic boom levels are explained in this section. Starting from flying the aircraft at the cut-off Mach number overland, the most promising projects and design concepts for low-boom aircraft are revised. In the last subsection, instead, exotic systems and technologies ideas worth exploring are also introduced.

According to the authors, among the unconventional configurations presented that could be adopted as the baseline, it is worth mentioning the oblique wing configuration, the supersonic biplane and the bi-directional flying wing.

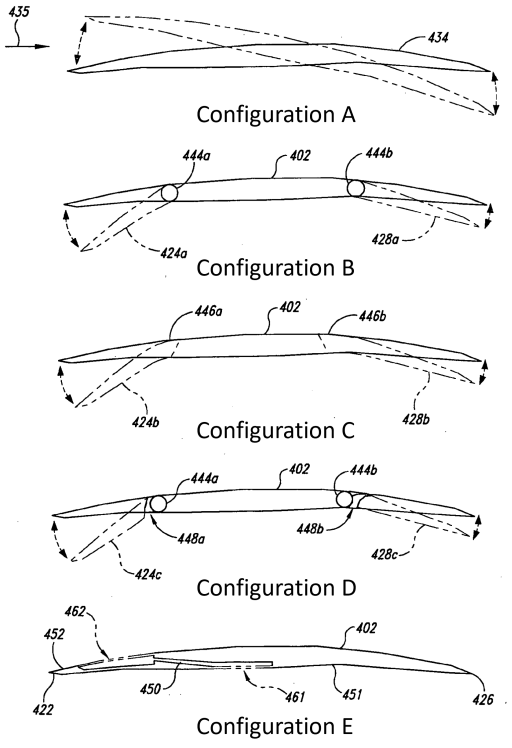

Figure 40. Various aerodynamic control devices that can be used to actively control lift distribution (Source: [232]).

Solution	Strengths	Limitations	TRL*
Nose Spike	Breaks single large nose shock into a series of weak shocks that will not coalesce into an N-wave. The system could be activated/deactivated on demand	Complexity of telescopic mechanism (high manufacturing costs and failure risk). Weight and power penalty.	8
Mechanical or eletrical shock wave dispersion	shock waves dispersion over a larger area to get lower pressure levels reaching the ground. Simple system (especially the mechanical version). The system could be activated and deactivated on demand.	Unfeasible for large scale applications. High deviation of the flow around the aircraft, increase of drag that requires an increase in propulsion power	2
Jet Stream	Interaction between high speed jet streams and wing shock wave could lead to a weakened wing shock and, under certain conditions, may improve the lift. Major portion of the anti-boom jet could be captured from the ambient atmosphere	Additional system to be added in the wing.	3
Flow suction and injection slots	Benefits in sonic boom and wave drag reduction. The system is passive, so no additiona power is required. Simplicity of operation and control. The system is effective also for off-design angles of attack.	The system cannot be activated / deactivated on demand.	3
Heating Addition	Sonic boom reduction by apparent increase of the airplane length (phantom body) created with the release of heat ahead of the body. The system could be activated / deactivated on demand.	The system requires extra power. Disturbace of the flow around the aircraft	2
Surface Cooling	Capability of controlling wave structures formation process up to large distance from the body by cooling the surface of shock waves nucleation.	The system cannot be activated / deactivated on demand. The system requires extra power. Weight penalty by addition of surface	2
Leading edge strake flap	Simple leading edge flap that can be deflected up and down to control sonic boom signature by shifting the lift distribution and shape the area distribution. The system could also be controlled to reduce lift ahead of spillage area. The system could be activated/deactivated on demand. The system is effective also for off design conditions.	Weight penalty due to actuators. Additional power required.	2
Leading edge and trailing edge flap	Simple leading edge- trailing edge flap system that can be deflected up and down to control sonic boom signature by shifting the lift distribution and shape the area distribution. The system could be used in high-boom mode optimizing aerodynamics performance at low speeds and in low boom mode in supersonic cruise. The system could be activated/deactivated on demand and easily controlled by the flight control system.	Weight penalty due to actuators. Additional power required.	3
***based on NASA definition**			

Figure 41. Sonic boom reduction systems and technologies summary table.

The oblique wing by Jones would, first of all, offer great aerodynamic performance with respect to a comparable symmetric configuration. In addition, since the equivalent area distribution of the wing would be better spread out longitudinally, this configuration would also mitigate sonic boom. According to some works, the overpressure level at the ground could result in one third of a comparable symmetric configuration, due to the cancellation of the aft-shock thanks to the favorable volume lift interference. Many technical challenges are related to the oblique wing design, such as nonlinear aerodynamics, unusual inertial couplings, aeroelastics and stability and control problems, and complex propulsion integration.

The supersonic biplane proposed by Busemann is a configuration that could, in theory, eliminate 80% of shock waves thanks to the interference between them and the expansion waves (wave cancellation effect). Sonic booms could be eliminated by this effect, leading to a boomless configuration. Research on the Busemann supersonic biplane concept carried out at Tohoku University shows that the best overall results would be obtained by coupling a supersonic biplane wing with a twin body configuration. In particular, sonic boom performance would reach acceptable values of both overpressure and loudness, with the best configuration having a maximum pressure rise 38% lower than the conventional single-body/diamond-wedge wing configuration. However, the wave cancellation effect would be not efficient at off-design conditions due to choked flow and hysteresis problems.

In the end, the supersonic bi-directional flying wing represents the revolutionary concept intended to break the technical barriers of conventional supersonic designs. According to Professor Zha and his group at University of Miami, it could, in fact, virtually fly with zero sonic booms and ultra-high aerodynamic efficiency in both supersonic and subsonic conditions. The flying wing is expected to rotate 90 deg passing from supersonic to subsonic mod, in order to achieve a lower sweep angle and high aspect ratio. The yaw moment to rotate the airframe would be generated by the ailerons or the flaps mounted on the two sides of the flying wing. This would avoid the need of a dedicated power driven system along with its weight and complexity penalty. Preliminary CFD simulations on a business jet version of this concept have shown no sonic booms generated for usual cruise Mach numbers (1.6,2). Maximum overpressure at the ground has been estimated to be 0.3 psf at the design angle of attack, and 0.9 psf for a cruising angle of attack to provide optimal L/D.

In this regard, one of the most promising concepts is the Gulfstream Aerospace patented Quiet Spike. It is an extendable nose spike developed to alter the shock wave field ahead of the aircraft. It works by breaking up the single large nose shock into a stair-stepped series of discrete small shocks. The Quiet Spike was adapted to an F-15B flight research aircraft and a total of 32 research flights were conducted that showed that it is possible to achieve a 0.2 psf initial shock reduction and an increase of 25% in rise time. The main drawbacks associated with this system are related to the complexity of the telescopic design, the weight and power penalty, the higher manufacturing costs and the failure risks. Another interesting concept for noise reduction is the shock wave dispersion. This technology aims to disperse shock waves over a larger area to have lower pressure levels at the ground. The dispersion is achieved by means of low-amplitude vibration of the aircraft nose, wing and tail leading edges obtained mechanically or electrically. Tests showed that through dispersion, especially for Mach numbers between 1 and 1.8, the footprint could be enlarged about 23 times. According to [213], shock wave dispersion represents a concrete alternative for shaping technology, having as a main disadvantage the high deviation of air stream around the aircraft that would require an increase in propulsion power.

In the end, in 2021, another reduction concept was presented by Ye et al. [224]. The idea consists of equipping the wing leading edge with a suction slot and the trailing edge with an injection slot. The result of several numerical and wind tunnel tests carried out on a diamond airfoil showed that the suction–injection device has benefits in both sonic boom and wave drag reduction, avoiding the weight penalty and reduction in fuselage space. Furthermore, it can be easily controlled by the flight control system, and switched on

just when required (over-cities supersonic flight). Other than the ones cited here, there are other promising noise reduction concepts worth mentioning, described in the respective subsections of the section.

For what it concerns, instead, the exotic systems and devices being tested or already patented, the most interesting ones seem to be the Quiet Spike nose, the shock wave dispersion obtained by membrane vibration, and the control lift devices. The Quiet Spike nose has been already largely tested in flight, showing good results, and for this reason represents the most mature technology. Its implementation remains still quite challenging due to the complexity of the telescopic structure that could raise also safety problems. The shock waves dispersion obtained by means of a vibrating membrane seems also feasible to be applied in the future on the leading edge of future supersonic wings. However, additional power would required to vibrate the membrane at a specific frequency, and a specific control system should be developed in order to activate the system and to run it at the right frequency to be effective at certain flight conditions. In the end, since control lift devices are already in plan on every aircraft, this solution could constitute the less demanding one. Of course, the effectiveness of the system should be demonstrated in flight, and flight control system should be tuned to recognize flight phases in which a high- or low-boom mode is required.

4. Conclusions

In this review, state-of-the-art literature on sonic boom prediction methods and reduction solutions was scrutinized to identify the main future challenges and opportunities for the design of the next generation of civil supersonic aircraft. Sonic boom fundamental theory, with its assumptions and limitations, was described, along with modern methods for sonic boom signature modeling and prediction. Near-field signature with accurate location and strengths of shock waves can be predicted by using techniques of different levels of fidelity, such as panel methods or computational fluid dynamics, in accordance with the design phase. Propagation to the ground can be conducted by optionally taking or not taking into account several atmospheric factors, such as molecular relaxation, turbulence, pressure and temperature gradients, etc. Regarding instead the effective reduction in the sonic boom levels produced by an aircraft in supersonic flight, flight operations, aircraft shape optimization techniques and active/passing systems and technologies are described as a solution. Ultimately, promising aircraft concepts and ongoing projects, as well as unconventional configurations, are also worthy of attention since a total breakthrough technology could result to be needed to fly supersonic overland without restrictions, paving the way to a new era of civil supersonic flight.

Author Contributions: Conceptualization, investigation, resources, writing, G.B.; supervision, review, C.L. and A.R.; funding acquisition, C.L. All authors have read and agreed to the published version of the manuscript.

Funding: This research was funded by the European Union's Horizon 2020 research and innovation program SENECA under grant agreement ID 101006742 DOI10.3030/101006742.

Conflicts of Interest: The authors declare no conflict of interest. The founders had no role in the study.

References

1. National, S.; Museum, S. Available online: https://airandspace.si.edu/collection-objects/bell-x-1 (accessed on 18 October 2023).
2. Gibbs, Y. Nasa Armstrong Fact Sheet: Sonic Booms. Available online: https://www.nasa.gov/centers/armstrong/news/FactSheets/FS-016-DFRC.html (accessed on 18 October 2023).
3. Coulouvrat, F. The challenges of defining an acceptable sonic boom overland. In Proceedings of the 15th AIAA/CEAS Aeroacoustics Conference (30th AIAA Aeroacoustics Conference), Miami, FL, USA, 11–13 May 2009; p. 3384.
4. Manci, K.M. *Effects of Aircraft Noise and Sonic Booms on Domestic Animals and Wildlife: A Literature Synthesis*; US Fish and Wildlife Service, National Ecology Research Center: Oxford, OH, USA, 1988; Volume 88.
5. Darden, C.M. Sonic boom theory: Its status in prediction and minimization. *J. Aircr.* **1977**, *14*, 569–576. [CrossRef]
6. FAQBite. What is a Sonic Boom? Available online: https://faqbite.com/what/what-is-a-sonic-boom/ (accessed on 18 October 2023).

7. Mabry, J.; Oncley, P. *Establishing Certification/Design Criteria for Advanced Supersonic Aircraft Utilizing Acceptance, Interference, and Annoyance Response to Simulated Sonic Booms by Persons in Their Homes*; Technical Report; Man-Acoustics And Noise Inc.: Seattle, WA, USA, 1973.
8. Liu, S.R.; Tong, B. International Civil Aviation Organization Supersonic Task Group overview and status. *J. Acoust. Soc. Am.* **2017**, *141*, 3566–3566. [CrossRef]
9. FAA. Supersonic Flight. Available online: https://www.faa.gov/newsroom/supersonic-flight?newsId=22754 (accessed on 18 October 2023).
10. Plotkin, K.J. State of the art of sonic boom modeling. *J. Acoust. Soc. Am.* **2002**, *111*, 530–536. [CrossRef] [PubMed]
11. Abraham, T.A. Sonic Boom Loudness Reduction Through Localized Supersonic Aircraft Equivalent-Area Changes. Ph.D Thesis, Utah State University, Logan, UT, USA, 2021.
12. Whitham, G.B. The flow pattern of a supersonic projectile. *Commun. Pure Appl. Math.* **1952**, *5*, 301–348. [CrossRef]
13. Whitham, G. On the propagation of weak shock waves. *J. Fluid Mech.* **1956**, *1*, 290–318. [CrossRef]
14. Hayes, W.D. Linearized supersonic flow. Ph.D Thesis, California Institute of Technology, Pasadena, CA, USA, 1947.
15. Jones, R. *Theory of Wing-Body Drag at Supersonic Speeds*; (No. NACA-TR-1284); NASA: Washington, DC, USA, 1956.
16. Whitcomb, R.T.; Fiscetti, T.L. *Development of a Supersonic Area Rule and an Application to the Design of a Wing-Body Combination Having High Lift-to-Drag Ratios*; (No. NACA-RM-L53H31a); NASA: Washington, DC, USA, 1956 1953.
17. Blokhintzev, D. The propagation of sound in an inhomogeneous and moving medium I. *J. Acoust. Soc. Am.* **1946**, *18*, 322–328. [CrossRef]
18. Carlson, H.W.; Maglieri, D.J. Review of sonic-boom generation theory and prediction methods. *J. Acoust. Soc. Am.* **1972**, *51*, 675–685. [CrossRef]
19. Lomax, H. *The Wave Drag of Arbitrary Configurations in Linearized Flow as Determined by Areas and Forces in Oblique Planes*; National Advisory Committee for Aeronautics: Hampton VA, USA, 1955.
20. Walkden, F. The shock pattern of a wing-body combination, far from the flight path. *Aeronaut. Q.* **1958**, *9*, 164–194. [CrossRef]
21. Carlson, H.W. *An Investigation of Some Aspects of the Sonic Boom by Means of Wind-Tunnel Measurements of Pressures about Several Bodies at a Mach Number of 2.01*; National Aeronautics and Space Administration: Hampton VA, USA, 1959; Volume 161.
22. Lina, L.J.; Maglieri, D.J. *Ground Measurements of Airplane Shock-Wave Noise at Mach Numbers to 2.0 and at Altitudes to 60,000 Feet*; National Aeronautics and Space Administration: Hampton VA, USA, 1960; Volume 235.
23. Smith, H.J. *Experimental and Calculated Flow Fields Produced by Airplanes Flying at Supersonic Speeds*; National Aeronautics and Space Administration: Hampton VA, USA, 1960; Volume 621.
24. Haefeli, R.; Hayes, W.; Kulsrud, H. *Sonic Boom Propagation in a Stratified Atmosphere, with Computer Program*; Technical Report; NASA: Hampton VA, USA, 1969.
25. THOMAS, C. *Extrapolation of Sonic Boom Pressure Signatures by the Waveform Parameter Method (Extrapolation of Sonic Boom Pressure Signatures by Waveform Parameter Method and Comparison with F-Function Method)*; No. A-4232; NASA: Washington, DC, USA, 1972.
26. Thomas, C.L. *Extrapolation of Wind-Tunnel Sonic Boom Signatures without Use of a Whitham F-Function*; NASA SP-255; NASA: Washington, DC, USA, 1970; pp. 205–217.
27. Plotkin, K.J.; Downing, M.; Page, J. USAF single event sonic boom prediction model: PCBOOM. *J. Acoust. Soc. Am.* **1994**, *95*, 2839–2839. [CrossRef]
28. Plotkin, K.J. *Pcboom3 Sonic Boom Prediction Model-Version 1.0 c*; Technical Report; Wyle Research Lab.: Arlington, VA, USA, 1996.
29. George, A.; Plotkin, K. Sonic Boom Amplitudes and Waveforms in a Real Atmosphere. *AIAA J.* **1969**, *7*, 1978–1981. [CrossRef]
30. Carlson, H.W. *Simplified Sonic-Boom Prediction*; Technical Report; NASA: Hampton VA, USA, 1978.
31. Scarselli, G.; Marulo, F.; Averardo, M.; Cafiero, A.; Selmin, V. Numerical comparison between a siimplified method and a full CFD approach for sonic boom evaluation on supersonic innovative configurations. In Proceedings of the 13th AIAA/CEAS Aeroacoustics Conference (28th AIAA Aeroacoustics Conference), Southampton, UK, 14–17 June 2022; p. 3675.
32. Clare, A.; Oman, R. Sonic Boom Prediction: A New Empirical Formulation and Animated Graphical Model. In *Transformational Science And Technology For The Current And Future Force: (With CD-ROM)*; World Scientific: Singapore, 2006; pp. 565–572.
33. Lee, R.; Downing, J. *Sonic Booms Produced by United States Air Force and United States Navy Aircraft: Measured Data*; Technical Report; Armstrong Lab.: Brooks Afb, TX, USA, 1991.
34. Plotkin, K. Review of sonic boom theory. In Proceedings of the 12th Aeroacoustic Conference, San Antonio,TX, USA, 10–12 April 1989; p. 1105.
35. McLean, F.E. *Some Nonasymptotic Effects on the Sonic Boom of Large Airplanes*; National Aeronautics and Space Administration: Hampton, VA, USA, 1965; Volume 2877.
36. Jung, T.P.; Starkey, R.P.; Argrow, B. Modified linear theory sonic booms compared to experimental and numerical results. *J. Aircr.* **2015**, *52*, 1821–1837. [CrossRef]
37. Page, J.; Plotkin, K. An efficient method for incorporating computational fluid dynamics into sonic boom prediction. In Proceedings of the 9th Applied Aerodynamics Conference, Baltimore, MD, USA, 23–25 September 1991; p. 3275.
38. Siclari, M.; Darden, C. Euler code prediction of near-field to midfield sonic boom pressure signatures. *J. Aircr.* **1993**, *30*, 911–917. [CrossRef]
39. Cheung, S.; Edwards, T.; Lawrence, S. Application of CFD to Sonic Boom Near and Mid flow-field prediction. In Proceedings of the 13th Aeroacoustics Conference, Washington, DC, USA, 5 June 1990; p. 3999.

40. Cliff, S.E.; Thomas, S.D. Euler/experiment correlations of sonic boom pressure signatures. *J. Aircr.* **1993**, *30*, 669–675. [CrossRef]
41. Wintzer, M.; Ordaz, I. Under-Track CFD-Based Shape Optimization for a Low-Boom Demonstrator Concept. In Proceedings of the 33rd AIAA Applied Aerodynamics Conference, Dallas, TX, USA, 22–26 June 2015; p. 2260.
42. Heath, C.M.; Slater, J.W.; Rallabhandi, S.K. Inlet trade study for a low-boom aircraft demonstrator. *J. Aircr.* **2017**, *54*, 1283–1293. [CrossRef]
43. Plotkin, K.; Page, J. Extrapolation of sonic boom signatures from CFD solutions. In Proceedings of the 40th AIAA Aerospace Sciences Meeting & Exhibit, Reno, NV, USA, 14–17 January 2002; p. 922.
44. Rallabhandi, S.K.; Mavris, D.N. New computational procedure for incorporating computational fluid dynamics into sonic boom prediction. *J. Aircr.* **2007**, *44*, 1964–1971. [CrossRef]
45. Ordaz, I.; Li, W. Using CFD Surface Solutions to Shape Sonic Boom Signatures Propagated from Off-Body Pressure. In Proceedings of the 31st AIAA Applied Aerodynamics Conference, San Diego, CA, USA, 24–27 June 2013; p. 2660.
46. Giblette, T.; Hunsaker, D.F. Prediction of sonic boom loudness using high-order panel methods for the near-field solution. In Proceedings of the AIAA Scitech 2019 Forum, San Diego, CA, USA, 7–11 January 2019; p. 0605.
47. Ehlers, F.; Johnson, F.; Rubbert, P. A higher order panel method for linearized supersonic flow. In Proceedings of the 9th Fluid and PlasmaDynamics Conference, Williamsburg , VA, USA, July 1979; p. 381.
48. Choi, S.; Alonso, J.J.; Kroo, I.M. Two-level multifidelity design optimization studies for supersonic jets. *J. Aircr.* **2009**, *46*, 776–790. [CrossRef]
49. Chan, M.K.Y. *Supersonic Aircraft Optimization for Minimizing Drag and Sonic Boom*; Stanford University: Stanford, CA, USA, 2003.
50. Rallabhandi, S.; Mavris, D. Design and analysis of supersonic business jet concepts. In Proceedings of the 6th AIAA Aviation Technology, Integration and Operations Conference (ATIO), Wichita, Kansas, 25–27 September 2006; p. 7702.
51. Ueno, A.; Kanamori, M.; Makino, Y. Multi-fidelity low-boom design based on near-field pressure signature. In Proceedings of the 54th AIAA Aerospace Sciences Meeting, San Diego, CA, USA, 4–8 January 2016; p. 2033.
52. Rallabhandi, S.K. Advanced sonic boom prediction using the augmented Burgers equation. *J. Aircr.* **2011**, *48*, 1245–1253. [CrossRef]
53. Cleveland, R.O. Propagation of Sonic Booms through a Real, Stratified Atmosphere. Ph.D. Thesis, The University of Texas at Austin, Austin, TX, USA, 1995.
54. Robinson, L.D. Sonic Boom Propagation through an Inhomogeneous, Windy Atmosphere. Ph.D. Thesis, The University of Texas at Austin, Austin, TX, USA, 1991.
55. Pilon, A.R. Spectrally accurate prediction of sonic boom signals. *AIAA J.* **2007**, *45*, 2149–2156. [CrossRef]
56. Lonzaga, J.B. Recent Enhancements to NASAâ€™s PCBoom Sonic Boom Propagation Code. In Proceedings of the AIAA Aviation 2019 Forum, Dallas, TX, USA, 17–21 June 2019; p. 3386.
57. Yamamoto, M.; Hashimoto, A.; Aoyama, T.; Sakai, T. A unified approach to an augmented Burgers equation for the propagation of sonic booms. *J. Acoust. Soc. Am.* **2015**, *137*, 1857–1866. [CrossRef]
58. Ozcer, I. Sonic boom prediction using Euler/full potential methodology. In Proceedings of the 45th AIAA Aerospace Sciences Meeting and Exhibit, Reno, NV, USA, 8–11 January 2007; p. 369.
59. Stout, T.A. Simulation of N-Wave and Shaped Supersonic Signature Turbulent Variations. Ph.D. Thesis, The Pennsylvania State University, State College, PA, USA, 2018.
60. Crow, S. Distortion of sonic bangs by atmospheric turbulence. *J. Fluid Mech.* **1969**, *37*, 529–563. [CrossRef]
61. Pierce, A.D. Statistical theory of atmospheric turbulence effects on sonic-boom rise times. *J. Acoust. Soc. Am.* **1971**, *49*, 906–924. [CrossRef]
62. Pierce, A.D.; Maglieri, D.J. Effects of atmospheric irregularities on sonic-boom propagation. *J. Acoust. Soc. Am.* **1972**, *51*, 702–721. [CrossRef]
63. Plotkin, K.J.; George, A. Propagation of weak shock waves through turbulence. *J. Fluid Mech.* **1972**, *54*, 449–467. [CrossRef]
64. Blanc-Benon, P.; Lipkens, B.; Dallois, L.; Hamilton, M.F.; Blackstock, D.T. Propagation of finite amplitude sound through turbulence: Modeling with geometrical acoustics and the parabolic approximation. *J. Acoust. Soc. Am.* **2002**, *111*, 487–498. [CrossRef] [PubMed]
65. Averiyanov, M.; Blanc-Benon, P.; Cleveland, R.O.; Khokhlova, V. Nonlinear and diffraction effects in propagation of N-waves in randomly inhomogeneous moving media. *J. Acoust. Soc. Am.* **2011**, *129*, 1760–1772. [CrossRef] [PubMed]
66. Bradley, K.A.; Hobbs, C.M.; Wilmer, C.B.; Sparrow, V.W.; Stout, T.A.; Morgenstern, J.M.; Underwood, K.H.; Maglieri, D.J.; Cowart, R.A.; Collmar, M.T.; et al. *Sonic Booms in Atmospheric Turbulence (SONICBAT): The Influence of Turbulence on Shaped Sonic Booms*; No. NASA/CR–2020–220509); NASA: Washington, DC, USA, 2020.
67. Locey, L.L. *Sonic Boom Postprocessing Functions to Simulate Atmospheric Turbulence Effects*; The Pennsylvania State University: State College, PA, USA, 2008.
68. Luquet, D. 3D Simulation of Acoustical Shock Waves Propagation through a Turbulent Atmosphere. Application to Sonic Boom. Ph.D Thesis, Université Pierre et Marie Curie, Paris, France, 2016.
69. Dagrau, F.; Rénier, M.; Marchiano, R.; Coulouvrat, F. Acoustic shock wave propagation in a heterogeneous medium: A numerical simulation beyond the parabolic approximation. *J. Acoust. Soc. Am.* **2011**, *130*, 20–32. [CrossRef]

70. Kanamori, M.; Takahashi, T.; Naka, Y.; Makino, Y.; Takahashi, H.; Ishikawa, H. Numerical Evauation of Effect of Atmospheric Turbulence on Sonic Boom Observed in D-SEND# 2 Flight Test. In Proceedings of the 55th AIAA Aerospace Sciences Meeting, Grapevine, TX, USA, 9–13 January 2017; p. 0278.
71. Kanamori, M.; Takahashi, T.; Ishikawa, H.; Makino, Y.; Naka, Y.; Takahashi, H. Numerical Evaluation of Sonic Boom Deformation due to Atmospheric Turbulence. *AIAA J.* **2021**, *59*, 972–986. [CrossRef]
72. Leconte, R.; Marchiano, R.; Coulouvrat, F.; Chassaing, J.C. Influence of atmospheric turbulence parameters on the propagation of sonic boom. In Proceedings of the Forum Acusticum, Lyon, France, 7–11 December 2021; pp. 979–980.
73. Kandil, O.; Ozcer, I.; Khasdeo, N. Sonic Boom Prediction, Focusing, and Mitigation. In Proceedings of the 2S Congress of the Aeronautical Sciences 2006, Hamburg, Germany, 3–8 September 2006.
74. Griffiths, G.W.; Schiesser, W.E. Linear and nonlinear waves. *Scholarpedia* **2009**, *4*, 4308. [CrossRef]
75. Van Hove, B.; Lofqvist, M.; Bonetti, D.; Kokorich, M. Reducing the Noise of Hypersonic Aircraft. 2023. Available online: https://www.researchgate.net/publication/367966282_Reducing_the_Noise_of_Hypersonic_Aircraft (accessed on 18 October 2023).
76. Guiraud, J.P. Acoustique geometrique bruit balistique des avions supersoniques et focalisation. *J. Mec.* **1965**, *4*, 215.
77. Seebass, R. *Nonlinear Acoustic Behavior at a Caustic*; Technical Report; Boeing Scientific Research Labs.: Seattle, WA, USA, 1971.
78. Gill, P.; Seebass, A. Nonlinear Acoustic Behavior at a Caustic-An Approximate Analytical Solution; In: *Aeroacoustics: Fan*; MIT Press: Cambridge, MA, USA, 1975; pp. 353–386.
79. Plotkin, K.; Cantril, J. Prediction of sonic boom at a focus. In Proceedings of the 14th Aerospace Sciences Meeting, Washington, DC, USA, 26–28 January 1976; p. 2.
80. Marchiano, R.; Coulouvrat, F.; Grenon, R. Numerical simulation of shock wave focusing at fold caustics, with application to sonic boom. *J. Acoust. Soc. Am.* **2003**, *114*, 1758–1771. [CrossRef]
81. Auger, T.; Coulouvrat, F. Numerical simulation of sonic boom focusing. *AIAA J.* **2002**, *40*, 1726–1734. [CrossRef]
82. Kandil, O.; Zheng, X. Prediction of Superboom Problem Using Computational Solution of Nonlinear Tricomi Equation. In Proceedings of the AIAA Atmospheric Flight Mechanics Conference and Exhibit, San Francisco, CA, USA, 15–18 August 2005; p. 6335.
83. Kandil, O.; Zheng, X. Computational solution of nonlinear Tricomi equation for sonic boom focusing and applications. In Proceedings of the AIP Conference Proceedings. American Institute of Physics, Mexico City, Mexico, 10–14 July 2006; Volume 838, pp. 607–610.
84. Piacsek, A.A. A Numerical Study of Weak Step Shocks That Focus in Two Dimensions. Ph.D. Thesis, The Pennsylvania State University, State College, PA, USA, 1995.
85. Piacsek, A.A. Atmospheric turbulence conditions leading to focused and folded sonic boom wave fronts. *J. Acoust. Soc. Am.* **2002**, *111*, 520–529. [CrossRef] [PubMed]
86. Loubeau, A. Recent progress on sonic boom research at NASA. In Proceedings of the INTER-NOISE and NOISE-CON Congress and Conference Proceedings. Institute of Noise Control Engineering, New York City, NY, USA, 19–22 August 2012; Volume 2012, pp. 3760–3770.
87. Taylor, A.D. *The TRAPS Sonic Boom Program*; Department of Commerce, National Oceanic and Atmospheric Administration: Washington, DC, USA, 1980; Volume 87.
88. Rallabhandi, S.; Fenbert, J. Numerical simulation of sonic boom focusing and its application to mission performance. *J. Acoust. Soc. Am.* **2017**, *141*, 3566–3566. [CrossRef]
89. E. U. Rumble. H2020. Available online: https://rumble-project.eu/i/dissemination/conference-presentations (accessed on 18 October 2023).
90. Töpken, S.; van de Par, S. Loudness and short-term annoyance of sonic boom signatures at low levels. *J. Acoust. Soc. Am.* **2021**, *149*, 2004–2015. [CrossRef] [PubMed]
91. Marshall, A.; Davies, P. A semantic differential study of low amplitude supersonic aircraft noise and other transient sounds. In Proceedings of the International Congress on Acoustics, Madrid, Spain, 2–7 September 2007; pp. 1–6.
92. Marshall, A.; Davies, P. A comparison of perceptual attributes and ratings of environmental transient sounds in two different playback environments. In Proceedings of the INTER-NOISE and NOISE-CON Congress and Conference Proceedings. Institute of Noise Control Engineering, Shanghai, China, 26–29 October 2008; Volume 2008, pp. 5586–5592.
93. Marshall, A.; Davies, P. Metrics including time-varying loudness models to assess the impact of sonic booms and other transient sounds. *Noise Control. Eng. J.* **2011**, *59*, 681–697. [CrossRef]
94. Glasberg, B.R.; Moore, B.C. A model of loudness applicable to time-varying sounds. *J. Audio Eng. Soc.* **2002**, *50*, 331–342.
95. Zwicker, E.; Fastl, H. *Psychoacoustics: Facts and Models*; Springer Science & Business Media: Berlin, Germany, 2013; Volume 22.
96. Maglieri, D.J.; Huckel, V.; Henderson, H.R. *Variability in Sonic Boom Signatures Measured Along an 8000-Foot Linear Array*; National Aeronautics and Space Administration: Washington, DC, USA, 1969; Volume 5040.
97. Doebler, W.J.; Sparrow, V.W. Stability of sonic boom metrics regarding signature distortions from atmospheric turbulence. *J. Acoust. Soc. Am.* **2017**, *141*, EL592–EL597. [CrossRef]
98. Leatherwood, J.D.; Sullivan, B.M. *Loudness and Annoyance Response to Simulated Outdoor and Indoor Sonic Booms*; No. NASA-TM-107756; NASA: Washington, DC, USA, 1993.
99. Stevens, S.S. Perceived level of noise by Mark VII and decibels (E). *J. Acoust. Soc. Am.* **1972**, *51*, 575–601. [CrossRef]

100. Borsky, P.N.; York, N.O.R.C.N. *Community Reactions to Sonic Booms in the Oklahoma City Area: Volume 2. Data on Community Reactions and Interpretations*; Aerospace Medical Research Laboratories: Brooks AFB, TX, USA, 1965.
101. Clarkson, B.L.; Mayes, W.H. Sonic-Boom-Induced Building Structure Responses Including Damage. *J. Acoust. Soc. Am.* **1972**, *51*, 742–757. [CrossRef]
102. Sizov, N.V.; Plotkin, K.J.; Hobbs, C.M. Predicting transmission of shaped sonic booms into a residential house structure. *J. Acoust. Soc. Am.* **2010**, *127*, 3347–3355. [CrossRef]
103. Minelli, A. Aero-Acoustic Shape Optimization of a Supersonic Business Jet. Ph.D. Thesis, Université Nice Sophia Antipolis, Nice, France, 2013.
104. Jones, L. Lower bounds for sonic bangs. *Aeronaut. J.* **1961**, *65*, 433–436. [CrossRef]
105. Carlson, H.W. *The Lower Bound of Attainable Sonic-Boom Overpressure and Design Methods of Approaching This Limit*; National Aeronautics and Space Administration: Washington, DC, USA, 1962.
106. Carlson, H.W. Influence of airplane configuration on sonic-boom characteristics. *J. Aircr.* **1964**, *1*, 82–86. [CrossRef]
107. Darden, C.M.; Powell, C.A.; Hayes, W.D.; George, A.R.; Pierce, A.D. Status of sonic boom methodology and understanding. In Proceedings of the Sonic Boom Workshop, Hampton, VA, USA, 1 June 1989.
108. George, A.; Seebass, R. Sonic boom minimization including both front and rear shocks. *AIAA J.* **1971**, *9*, 2091–2093. [CrossRef]
109. Seebass, R.; George, A.R. Sonic-Boom Minimization. *J. Acoust. Soc. Am.* **1972**, *51*, 686–694. [CrossRef]
110. Darden, C.M. *Sonic-Boom Minimization with Nose-Bluntness Relaxation*; National Aeronautics and Space Administration, Scientific and Technical: Washington, DC, USA, 1979; Volume 1348.
111. Carlson, H.W.; Barger, R.L.; Mack, R.J. *Application of Sonic-Boom Minimization Concepts in Supersonic Transport Design*; No. NASA-TN-D-7218; NASA: Washington, DC, USA, 1973.
112. Mack, R.J. *Wind-Tunnel Investigation of the Validity of a Sonic-Boom-Minimization Concept*; NASA TP D-1421 ; NASA: Washington, DC, USA, 1979.
113. Mack, R.J.; Needleman, K.E. *A Methodology for Designing Aircraft to Low Sonic Boom Constraints*; Technical Report; NASA: Washington, DC, USA, 1991.
114. Rallabhandi, S.K.; Mavris, D.N. Aircraft geometry design and optimization for sonic boom reduction. *J. Aircr.* **2007**, *44*, 35–47. [CrossRef]
115. Plotkin, K.; Rallabhandi, S.; Li, W. Generalized formulation and extension of sonic boom minimization theory for front and aft shaping. In Proceedings of the 47th AIAA Aerospace Sciences Meeting including The New Horizons Forum and Aerospace Exposition, Orlando, FL, USA, 5–8 January 2009; p. 1052.
116. Jung, T.P.; Starkey, R.P.; Argrow, B. Lobe balancing design method to create frozen sonic booms using aircraft components. *J. Aircr.* **2012**, *49*, 1878–1893. [CrossRef]
117. Farhat, C.; Argrow, B.; Nikbay, M.; Maute, K. Shape optimization with F-function balancing for reducing the sonic boom initial shock pressure rise. *Int. J. Aeroacoustics* **2004**, *3*, 361–377. [CrossRef]
118. Minelli, A.; Salah el Din, I.; Carrier, G. Inverse design approach for low-boom supersonic configurations. *AIAA J.* **2014**, *52*, 2198–2212. [CrossRef]
119. Wintzer, M.; Kroo, I.; Aftosmis, M.; Nemec, M. Conceptual design of low sonic boom aircraft using adjoint-based CFD. In Proceedings of the Seventh International Conference on Computational Fluid Dynamics (ICCFD7), Big Island, HI, USA, 9–13 July 2012.
120. Feng, X.; Li, Z.; Song, B. Research of low boom and low drag supersonic aircraft design. *Chin. J. Aeronaut.* **2014**, *27*, 531–541. [CrossRef]
121. Li, W.; Rallabhandi, S. Inverse design of low-boom supersonic concepts using reversed equivalent-area targets. *J. Aircr.* **2014**, *51*, 29–36. [CrossRef]
122. Zhang, Y.; Huang, J.; Zhenghong, G.; Chao, W.; Bowen, S. Inverse design of low boom configurations using proper orthogonal decomposition and augmented Burgers equation. *Chin. J. Aeronaut.* **2019**, *32*, 1380–1389. [CrossRef]
123. Li, W.; Geiselhart, K. Multidisciplinary design optimization of low-boom supersonic aircraft with mission constraints. *AIAA J.* **2021**, *59*, 165–179. [CrossRef]
124. Goel, N.; Jawahar, S. Towards a Supersonic Transport: Minimization of Sonic Boom. *J. Stud. Res.* **2022**, *11*. 1/jsrhs.v11i3.3391. [CrossRef]
125. Maglieri, D.J.; Bobbitt, P.J.; Plotkin, K.J.; Shepherd, K.P.; Coen, P.G.; Richwine, D.M. *Sonic Boom: Six Decades of Research*; Special Publication (SP); NASA: Washington, DC, USA, 2014.
126. Oceanic, U.S.N.; Administration, A.; Force, U.S.A. *US Standard Atmosphere, 1976*; National Oceanic and Atmospheric Administration: Washington, DC, USA, 1976; Volume 76.
127. Page JA, L.A. Aircraft Noise Generation and Assessment Section 5-Overall Vehicle System Noise, Part d-Sonic Boom. *CEAS Aeronaut J.* **2019**, *10*, 335–353. [CrossRef] [PubMed]
128. Cliatt, L.J.; Hill, M.A.; Haering, E. Mach cutoff analysis and results from NASA's Farfield investigation of no-boom thresholds. In Proceedings of the 22nd AIAA/CEAS Aeroacoustics Conference, Lyon, France, 30 May–1 July 2016; p. 3011.
129. Haering, E.A., Jr.; Smolka, J.W.; Murray, J.E.; Plotkin, K.J. Flight Demonstration Of Low Overpressure N-Wave Sonic Booms and Evanescent Waves. In Proceedings of the AIP American Institute of Physics, Mexico City, Mexico, 10–14 July 2006; Volume 838, pp. 647–650.

130. Wlezien, R.; Veitch, L. Quiet Supersonic Platform Program Advanced algorithms for design and optimization of Quiet Supersonic Platforms. In Proceedings of the 40th AIAA Aerospace Sciences Meeting & Exhibit, Reno, NV, USA, 14–17 January 2002; p. 143.
131. Security, G. Quiet Supersonic Platform (qsp). Available online: https://www.globalsecurity.org/military/systems/aircraft/qsp.htm (accessed on 18 October 2023).
132. Komadina, S.; Drake, A.; Bruner, S. Development of a quiet supersonic aircraft with technology applications to military and civil Aircraft. In Proceedings of the 40th AIAA Aerospace Sciences Meeting & Exhibit, Reno, NV, USA, 14–17 January 2002; p. 519.
133. NASA. Quiet Spike Project. Available online: https://www.nasa.gov/centers/dryden/multimedia/imagegallery/Quiet_Spike/Quiet_Spike_proj_desc.html (accessed on 18 October 2023).
134. NASA. Shaped Sonic Boom Demonstration. Available online: https://www.nasa.gov/centers/dryden/multimedia/imagegallery/SSBD/SSBD_proj_desc.html (accessed on 18 October 2023).
135. NASA. Nasa Investigates the 'Faint' Side of Sonic Booms. Available online: https://www.nasa.gov/topics/aeronautics/features/faint_sonic_booms.html (accessed on 18 October 2023).
136. NASA. Nasa Quiet Sonic Boom Research Effort Ends with a Whisper. Available online: https://www.nasa.gov/centers/dryden/Features/WSPR_research_complete.html (accessed on 18 October 2023).
137. Wikipedia. Available online: https://en.wikipedia.org/wiki/Gulfstream_X-54 (accessed on 18 October 2023).
138. NASA. Nasa Chat: Taking the "Boom" Out of Booms. Available online: https://www.nasa.gov/connect/chat/sonic_boom_chat.html (accessed on 18 October 2023).
139. Security, G. X-54 Relaxed Isentropic Compression. Available online: https://www.globalsecurity.org/military/systems/aircraft/x-54.htm (accessed on 18 October 2023).
140. JAXA. D-Send Project(fy2010-fy2015). Available online: https://www.aero.jaxa.jp/eng/research/frontier/sst/d-send.html (accessed on 18 October 2023).
141. Sakata, K. Japan's supersonic technology and business jet perspectives. In Proceedings of the 51st AIAA Aerospace Sciences Meeting including the New Horizons Forum and Aerospace Exposition, Grapevine, TX, USA, 7–10 January 2013; p. 21.
142. Sakata, K. Challenge for Supersonic Business Jet SKY Mobility Innovation 10/12/12. Available online: https://www.skyaero.jp/ja/research/challenge4ssbj.pdf (accessed on 18 October 2023).
143. CORDIS. Environmentally Friendly High Speed Aircraft. Available online: https://cordis.europa.eu/project/id/516132 (accessed on 18 October 2023).
144. CORDIS. HISAC Project Publishable Activity Report; Technical Report; CORDIS: Hialeah, FL, USA, 2008.
145. CORDIS. Mdo and Regulations for Low-Boom and Environmentally Sustainable Supersonic Aviation. Available online: https://cordis.europa.eu/project/id/101006856 (accessed on 18 October 2023).
146. Piccirillo, G.; Graziani, S.; Fusaro, R.; Viola, N. Lto noise and sonic boom predictions in early conceptual design phases. In Proceedings of the ICAS 2022, Stockholm, Sweden, 4–9 September 2022.
147. Rodriguez, D. Propulsion/Airframe integration and optimization on a supersonic business jet. In Proceedings of the 45th AIAA Aerospace Sciences Meeting and Exhibit, Reno, NV, USA, 8–11 January 2007; p. 1048.
148. Technology, A. The Aerion Super Sonic Business Jet Project, USA. Available online: https://www.aerospace-technology.com/projects/aerionsbjsupersonicb/ (accessed on 18 October 2023).
149. Masunaga, S. To Get Supersonic Business Jets off the Ground, Aerion Corp. Is Building Planes that Don't go 'Boom'. Available online: https://www.latimes.com/business/la-fi-supersonic-aerion-20180911-story.html (accessed on 18 October 2023).
150. Technology, A. Aerion as2 Supersonic Business Jet. Available online: https://www.aerospace-technology.com/projects/aerion-as2-supersonic-business-jet/ (accessed on 18 October 2023).
151. Sampson, B. Aerion Supersonic jet Developer Makes Key Appointments. Available online: https://www.businessairportinternational.com/news/aircraft/aerion-supersonic-jet-developer-makes-key-appointments.html (accessed on 18 October 2023).
152. Academy, A.S. From Concorde to New Supersonic Aircraft Projects-Dossier 46. Available online: https://academieairespace.com/wp-content/uploads/2019/06/AAE_D46_UK_WEB.pdf (accessed on 18 October 2023).
153. George, A. Supersonic Jet Ditches Windows for Massive Live-Streaming Screens. Available online: https://www.wired.com/2014/02/supersonic-jet-video-windows/ (accessed on 18 October 2023).
154. Aerospace, S. Quiet & Sustainable Supersonic Flight. Available online: https://www.spikeaerospace.com/s-512-supersonic-jet/quiet-supersonic-flight/ (accessed on 18 October 2023).
155. Technology, A. Spike s-512 Supersonic Business Jet. Available online: https://www.aerospace-technology.com/projects/spike-s-512-supersonic-business-jet/ (accessed on 18 October 2023).
156. Staff, F. Spike Aerospace s-512 Quiet Supersonic Commercial Business Jet. Available online: https://sofrep.com/fightersweep/spike-aerospace-s-512-quiet-supersonic-commercial-business-jet/ (accessed on 18 October 2023).
157. Supersonic, B. Supersonic Passenger Airplanes Boom Supersonic. 2020. Available online: https://boomsupersonic.com/ (accessed on 18 October 2023).
158. Wikipedia. Boom Technology. Available online: https://en.wikipedia.org/wiki/Boom_Technology (accessed on 18 October 2023).
159. Cook, M. Boom Enters Supersonic Air Force One Race. Available online: https://www.avweb.com/aviation-news/boom-enters-supersonic-air-force-one-race/ (accessed on 18 October 2023).
160. Guardian, T. United Airlines Aims to Revive Concorde Spirit with Supersonic Planes. Available online: https://www.theguardian.com/business/2021/jun/03/united-airlines-boom-supersonic-overture-airliner-concorde (accessed on 18 October 2023).

161. Supersonic, B. Overture. Available online: https://boomsupersonic.com/overture (accessed on 18 October 2023).
162. Banke, J. New Nasa x-Plane Construction Begins Now. Available online: https://www.nasa.gov/lowboom/new-nasa-x-plane-construction-begins-now (accessed on 18 October 2023).
163. Giangreco, L. Lockheed and Nasa Move toward Design Review for Supersonic x-Plane. Available online: https://www.flightglobal.com/helicopters/lockheed-and-nasa-move-toward-design-review-for-supersonic-x-plane/123441.article (accessed on 18 October 2023).
164. Week, G.N.A.; Technology, S. Final Testing Will Clear Way for Assembly of Supersonic x-59a. Available online: https://aviationweek.com/air-transport/final-testing-will-clear-way-assembly-supersonic-x-59a (accessed on 18 October 2023).
165. Gipson, L. Low-Boom Flight Demonstration. Available online: https://www.nasa.gov/mission_pages/lowboom/flights (accessed on 18 October 2023).
166. Proponet. Lockheed Martin Begins Manufacturing, Commits to 3-Year Timeline for x-59 Quesst Low-Boom Demonstrator. Available online: https://www.proponent.com/lockheed-martin-manufacturing-x-59-quesst-low-boom-demonstrator/ (accessed on 18 October 2023).
167. Wikipedia. Sai Quiet Supersonic Transport. Available online: https://en.wikipedia.org/wiki/SAI_Quiet_Supersonic_Transport#cite_note-popsci2007march-3 (accessed on 18 October 2023).
168. Hagerman, E. All Sonic, no Boom. Available online: https://www.popsci.com/military-aviation-space/article/2007-03/all-sonic-no-boom/ (accessed on 18 October 2023).
169. Trimble, S. Sai Resurrects Qsst-x as All-First Class Supersonic Airliner, Seeks Investors. Available online: https://www.flightglobal.com/sai-resurrects-qsst-x-as-all-first-class-supersonic-airliner-seeks-investors/110088.article (accessed on 18 October 2023).
170. International, S.A. Quiet Supersonic Transport-x. Available online: https://sai-qsstx.com/ (accessed on 18 October 2023).
171. Beautiful Life Online Magazine. Sai Quiet Supersonic Transport. Available online: https://www.beautifullife.info/automotive-design/sai-quiet-supersonic-transport/ (accessed on 18 October 2023).
172. CNN, J.B. Race to be First with 'Son of Supersonic'. Available online: http://edition.cnn.com/2011/TECH/innovation/06/21/concorde.hyper.sonic/index.html (accessed on 18 October 2023).
173. AINonline, L.M. Paris 2011: HYPERSONIC Hyperbole. Available online: https://www.ainonline.com/aviation-news/business-aviation/2011-06-21/paris-2011-hypersonic-hyperbole (accessed on 18 October 2023).
174. JetOptions. Hypermach Now Shooting for Mach 4.0 Business Jet. Available online: https://www.flyjetoptions.com/hypermach-now-shooting-for-mach-4-0-business-jet/ (accessed on 18 October 2023).
175. Darren, Q. Hypermach Unveils Sonicstar Supersonic Business Jet Concept. Available online: https://newatlas.com/hypermach-sonicstar-ssbj-concept/18974/ (accessed on 18 October 2023).
176. Security, G. Hypermach Aerospace Industries. Available online: https://www.globalsecurity.org/military/systems/aircraft/hypermach.htm (accessed on 18 October 2023).
177. Trautvetter, C. Hypermach at 'Pivotal Stage' for Its Mach 5 Bizjet. Available online: https://www.ainonline.com/aviation-news/business-aviation/2016-11-01/hypermach-pivotal-stage-its-mach-5-bizjet (accessed on 18 October 2023).
178. Gibbs, Y. Nasa Armstrong Fact Sheet: X-29 Advanced Technology Demonstrator Aircraft. Available online: https://www.nasa.gov/centers/armstrong/news/FactSheets/FS-008-DFRC.html (accessed on 18 October 2023).
179. Wikimedia. Sukhoi su-47 in 2008. Available online: https://commons.wikimedia.org/wiki/File:Sukhoi_Su-47_in_2008.jpg (accessed on 18 October 2023).
180. Winter, G. Kb Sat sr-10 ex-88004. Available online: https://www.flickr.com/photos/57931616@N03/36149040295 (accessed on 18 October 2023).
181. Kishi, Y.; Makino, Y.; Kanazaki, M. Numerical Investigation of Sonic Boom for Forward-Swept Wing Based on Euler and Augmented Burgers Equations. *Aerosp. Technol. Jpn. Jpn. Soc. Aeronaut. Space Sci.* **2020**, *19*, 1–9. [CrossRef]
182. Horinouchi, S. Variable Forward-Swept Wing Supersonic Aircraft Having Both Low-Boom Characteristics and Low-Drag Characteristics. U.S. Patent Application Number 11/103, 12 April 2005, p. 549.
183. Raymer,D. *Aircraft Design: A Conceptual Approach*; American Institute of Aeronautics and Astronautics Inc.: Reston, VA, USA, 1992; pp. 515–552.
184. Desktop Aeronautics *Oblique Flying Wings: An Introduction and White Paper*; Desktop Aeronautics: Palo Alto, CA, USA, 2005.
185. Filippone, A. The Oblique Flying Wing. Available online: https://aerodyn.org/ofw/ (accessed on 18 October 2023).
186. Conner, M. Nasa Armstrong Fact Sheet: The ad-1. Available online: https://www.nasa.gov/centers/armstrong/news/FactSheets/FS-019-AFRC.html (accessed on 18 October 2023).
187. Reddit. 1970s "Flying Oblique Wing" Concept, Designed by r.t. Jones, art by Rick Guidice, for NASA. Available online: https://www.reddit.com/r/RetroFuturism/comments/aw47jq/1970s_flying_oblique_wing_concept_designed_by_rt/ (accessed on 18 October 2023).
188. Hicks, R.M.; Mendoza, J.P. *Oblique-Wing Sonic Boom*; NASA: Washington, DC, USA, 1973.
189. Van der Velden, A.; Kroo, I. Sonic boom of the oblique flying wing. *J. Aircr.* **1994**, *31*, 19–25. [CrossRef]
190. El-Salamony, M. Oblique Flying Wing: Past and Future. In Proceedings of the Proceedings of Extremal and Record-Breaking Aircrafts Workshop (ERBA), Dolgoprudny, Russia, 5–15 July 2016.
191. Busemann, A. Aerodynamic lift at supersonic speeds. *Luftfahrtforschung* **1935**.
192. Kusunose, K.; Matsushima, K.; Maruyama, D. Supersonic biplane—A review. *Prog. Aerosp. Sci.* **2011**, *47*, 53–87. [CrossRef]

193. Hu, R.; Jameson, A.; Wang, Q. Adjoint-based aerodynamic optimization of supersonic biplane airfoils. *J. Aircr.* **2012**, *49*, 802–814. [CrossRef]
194. Licher, R. *Optimum Two-Dimensional Multiplanes in Supersonic Flow*; Douglas Aircraft Company: Santa Monica, CA, USA, 1955.
195. Ban, N.; Yamazaki, W.; Kusunose, K. Low-boom/low-drag design optimization of innovative supersonic transport configuration. *J. Aircr.* **2018**, *55*, 1071–1081. [CrossRef]
196. Maruyama, D.; Kusunose, K.; Matsushima, K.; Nakahashi, K. Numerical Analysis and Design of Supersonic Wings Based on Busemann Biplane. 2007. Available online: https://www.eucass.eu/component/docindexer/?task=download&id=2992 (accessed on 18 October 2023)
197. Yamashita, H.; Yonezawa, M.; Obayashi, S.; Kusunose, K. A study of busemann-type biplane for avoiding choked flow. In Proceedings of the 45th AIAA Aerospace Sciences Meeting and Exhibit, Reno, NV, USA, 8–11 January 2007; p. 688.
198. Maruyama, D.; Kusunose, K.; Matsushima, K. Aerodynamic characteristics of a two-dimensional supersonic biplane, covering its take-off to cruise conditions. *Shock Waves* **2009**, *18*, 437–450. [CrossRef]
199. Zhai, J.; Zhang, C.A.; Wang, F.M.; Zhang, W.W. Design of a new supersonic biplane. *Acta Astronaut.* **2020**, *175*, 216–233. [CrossRef]
200. Yonezawa, M.; Yamashita, H.; Obayashi, S.; Kusunose, K. Investigation of supersonic wing shape using Busemann biplane airfoil. In Proceedings of the 45th AIAA Aerospace Sciences Meeting and Exhibit, Reno, NV, USA, 8–11 January, 2007; p. 686.
201. Yonezawa, M.; Obayashi, S. Reducing drag penalty in the three-dimensional supersonic biplane. *Proc. Inst. Mech. Eng. Part J. Aerosp. Eng.* **2009**, *223*, 891–899. [CrossRef]
202. Yamashita, H.; Kuratani, N.; Yonezawa, M.; Ogawa, T.; Nagai, H.; Asai, K.; Obayashi, S. Wind tunnel testing on start/unstart characteristics of finite supersonic biplane wing. *Int. J. Aerosp. Eng.* **2013**, *2013*, 231434. [CrossRef]
203. Maruyama, D.; Kusunose, K.; Matsushima, K.; Nakahashi, K. Aerodynamic analysis and design of Busemann biplane: towards efficient supersonic flight. *Proc. Inst. Mech. Eng. Part J. Aerosp. Eng.* **2012**, *226*, 217–238. [CrossRef]
204. Utsumi, Y.; Obayashi, S. Design of supersonic biplane aircraft concerning sonic boom minimization. In Proceedings of the 28th AIAA Applied Aerodynamics Conference, Chicago, IL, USA, 28 June–1 July 2010; p. 4962.
205. Yamazaki, W.; Kusunose, K. Aerodynamic Study of Twin-Body Fuselage Configuration for Supersonic Transport. *Trans. Jpn. Soc. Aeronaut. Space Sci.* **2013**, *56*, 229–236. [CrossRef]
206. Yamazaki, W.; Kusunose, K. Aerodynamic/sonic boom performance evaluation of innovative supersonic transport configurations. *J. Aircr.* **2016**, *53*, 942–950. [CrossRef]
207. Anthony, S. Supersonic Biplanes: More Fuel Efficient, Quieter Sonic Booms. Available online: https://www.extremetech.com/extreme/133259-supersonic-biplanes-more-fuel-efficient-quieter-sonic-booms (accessed on 18 October 2023).
208. Yamazaki, W.; Kusunose, K. Innovative supersonic transport configuration by biplane wing/twin-body fuselage. In Proceedings of the 29th ICAS Congress, ICAS Paper, St. Petersburg, Russia, 7–12 September 2014; Volume 735, p. 2014.
209. Zha, G.; Im, H.; Espinal, D. Toward zero sonic-boom and high efficiency supersonic flight, part I: a novel concept of supersonic bi-directional flying wing. In Proceedings of the 48th AIAA Aerospace Sciences Meeting Including the New Horizons Forum and Aerospace Exposition, Orlando, FL, USA, 4–7 January 2010; p. 1013.
210. Espinal, D.; Lee, B.; Sposato, H.; Kinard, D.; Dominguez, J.; Zha, G.C.; Im, H. Supersonic bi-directional flying wing, Part II: Conceptual design of a high speed civil transport. In Proceedings of the 48th AIAA Aerospace Sciences Meeting Including the New Horizons Forum and Aerospace Exposition, Orlando, FL, USA, 4–7 January 2010; p. 1393.
211. Berger, C.; Carmona, K.; Espinal, D.; Im, H.; Zha, G. Supersonic bi-directional flying wing configuration with low sonic boom and high aerodynamic efficiency. In Proceedings of the 29th AIAA Applied Aerodynamics Conference, Reston, VA, USA, 27–30 June 2011; p. 3663.
212. Zha, G.; Cattafesta, L.; Alvi, F.S. *Silent and Efficient Supersonic Bi-Directional Flying Wing*; Final Report for NASA NIAC Phase I Grant NNX12AR05G8; NASA: Washington, DC, USA, 2013.
213. Sandu, C.; Sandu, R.C.; Olariu, C.T. Sonic Boom Mitigation through Shock Wave Dispersion. In *Environmental Impact of Aviation and Sustainable Solutions*; IntechOpen: London, UK, 2019.
214. Henne, P.A.; Howe, D.C.; Wolz, R.R.; Hancock, J.L., Jr. Supersonic Aircraft with Spike for Controlling and Reducing Sonic Boom. U.S. Patent 6,698,684, 22 March 2002.
215. Simmons, F.; Freund, D. Wing morphing for quiet supersonic jet performance-variable geometry design challenges for business jet utilization. In Proceedings of the 43rd AIAA Aerospace Sciences Meeting and Exhibit, Reno, NV, USA, 10–13 January 2005; p. 1017.
216. Howe, D. Improved sonic boom minimization with extendable nose spike. In Proceedings of the 43rd AIAA Aerospace Sciences Meeting and Exhibit, Reno, NV, USA, 10–13 January 2005; p. 1014.
217. Simmons, F.; Freund, D.; Spivey, N.; Schuster, L. Quiet spike: The design and validation of an extendable nose boom prototype. In Proceedings of the 48th AIAA/ASME/ASCE/AHS/ASC Structures, Structural Dynamics, and Materials Conference, Honolulu, HI, USA, 23–26 April 2007; p. 1774.
218. Sun, Y.; Smith, H. Review and prospect of supersonic business jet design. *Prog. Aerosp. Sci.* **2017**, *90*, 12–38. [CrossRef]
219. Freund, D.; Simmons, F.; Spivey, N.; Schuster, L. Quiet Spike Prototype Flight Test Results. In Proceedings of the 48th AIAA/ASME/ASCE/AHS/ASC Structures, Structural Dynamics, and Materials Conference, Honolulu, HI, USA, 23–26 April 2007; p. 1778.

220. Freund, D.; Simmons, F.; Howe, D.; Cowart, R.; Grindle, T. Lessons Learned-Quiet SpikeTM Flight Test Program. In Proceedings of the 46th AIAA Aerospace Sciences Meeting and Exhibit, Reno, NV, USA, 7–10 January 2008; p. 130.
221. Gulfstream Aerospace Corporation. An Overview of the Gulfstream An Overview of the Gulfstream Supersonic Technology Supersonic Technology Program. 2010. Available online: https://www.faa.gov/sites/faa.gov/files/about/office_org/headquarters_offices/apl/BaltimorePublicMeeting-Gulfstream.pdf (accessed on 18 October 2023).
222. Sandu, C.; Brasoveanu, D. New solution for sonic boom mitigation. Concept and testing methodology. Application at European supersonic business jet. In Proceedings of the 33-rd Caius Iacob Conference-Fluid Mechanics and Technical Applications, Bucharest, Romania, 29–30 September 2011; pp. 29–30.
223. Cheng, S. Device for Sonic Boom Reduction and Improving Aircraft Performance. U.S. Patent 3,737,119, 5 June 1973.
224. Ye, L.Q.; Ye, Z.Y.; Ye, K.; Wu, J.; Miao, S.J. A low-boom and low-drag design method for supersonic aircraft and its applications on airfoils. *Adv. Aerodyn.* **2021**, *3*, 1–27. [CrossRef]
225. Miles, R.B.; Martinelli, L.; Macheret, S.O.; Shneider, M.; Girgis, I.G.; Zaidi, S.H.; Mansfield, D.; Siclari, M.; Smereczniak, P.; Kashuba, R.; et al. Suppression of sonic boom by dynamic off-body energy addition and shape optimization. *AIAA Paper* **2002**, *150*, 33.
226. Zaidi, S.H.; Shneider, M.; Miles, R. Shock-wave mitigation through an off-body pulsed energy deposition. *AIAA J.* **2004**, *42*, 326–331. [CrossRef]
227. Potapkin, A.; Moskvichev, D.Y. Reduction of the sonic boom level by heating the flow in front of the body. *Shock Waves* **2014**, *24*, 429–437. [CrossRef]
228. Fomin, V.; Tretyakov, P. Active methods of affecting a supersonic flow. in: Advanced Problems of Science, Proceedings of the Scientific Session of the Siberian Division of the Russian Academy of Sciences and the Siberian Division of the Russian Academy of Medical Sciences, 25–26 November 2003, Nauka, Novosibirsk, pp. 185–208.
229. Shneyder, M.; Macheret, S.; Zaidi, S.; Girgis, I.; Miles, R. Steady and unsteady supersonic flow control with energy addition. In Proceedings of the 34th AIAA Plasmadynamics and Lasers Conference, Orlando, FL, USA, 23–26 June 2003; p. 3862.
230. Fomin, V.; Chirkashenko, V.; Volkov, V.; Kharitonov, A. Reduction of the sonic boom level in supersonic aircraft flight by the method of surface cooling. *Thermophys. Aeromech.* **2013**, *20*, 669–678. [CrossRef]
231. Morgenstern, J.M.; Arslan, A. Aircraft Lift Device for Low Sonic Boom. U.S. Patent 6,935,592, 30 August 2005.
232. Adamson, E.; Nelson, C. Supersonic Aircraft with Active Lift Distribution Control for Reducing Sonic Boom. U.S. Patent App. 11/039,651, 20 July 2006.

Review of sonic boom prediction and reduction methods for next generation of supersonic aircraft

Bonavolontà, Giordana

2023-11-01

Bonavolontà G, Lawson C, Riaz A. (2023) Review of sonic boom prediction and reduction methods for next generation of supersonic aircraft. Aerospace, Volume 10, Issue 11, November 2023, Article Number 917

https://doi.org/10.3390/aerospace10110917